



HAL
open science

Headwater Flow Geochemistry of Mount Everest (Upper Dudh Koshi River, Nepal)

Pierre Chevallier, Jean-luc Seidel, J.D. Taupin, Ornella Puschiasis

► **To cite this version:**

Pierre Chevallier, Jean-luc Seidel, J.D. Taupin, Ornella Puschiasis. Headwater Flow Geochemistry of Mount Everest (Upper Dudh Koshi River, Nepal). *Frontiers in Earth Science*, 2020, 8, 10.3389/feart.2020.00351 . hal-02988645

HAL Id: hal-02988645

<https://hal.umontpellier.fr/hal-02988645>

Submitted on 20 Nov 2020

HAL is a multi-disciplinary open access archive for the deposit and dissemination of scientific research documents, whether they are published or not. The documents may come from teaching and research institutions in France or abroad, or from public or private research centers.

L'archive ouverte pluridisciplinaire **HAL**, est destinée au dépôt et à la diffusion de documents scientifiques de niveau recherche, publiés ou non, émanant des établissements d'enseignement et de recherche français ou étrangers, des laboratoires publics ou privés.

Headwater Flow Geochemistry of Mount Everest (Upper Dudh Koshi River, Nepal)

1 **Pierre Chevallier^{1*}, Jean-Luc Seidel¹, Jean-Denis Taupin¹, Ornella Puschiasis²**

2 ¹Laboratoire HydroSciences Montpellier (CNRS, IRD, Université de Montpellier), Université de
3 Montpellier, 163, avenue Auguste Broussonnet, CC 57, 34090 Montpellier, France

4 ²Centre d'Etudes en Sciences Sociales sur les Mondes Africains, Américains et Asiatiques
5 (INALCO, Université de Paris, IRD), 65, rue des Grands Moulins, 75013 Paris, France; Associate
6 Scientist, Centre d'Etudes Himalayennes (CNRS)

7 *** Correspondence:**

8 Pierre Chevallier

9 pierre.chevallier@ird.fr

10 **Keywords: major ions, trace elements, stable isotopes, precipitation, river flow, water use,**
11 **Central Himalaya.**

12 **Abstract**

13 The aim of this work, conducted in the upper valley of the Khumbu on the southern part of Mount
14 Everest, is to approach in parallel **three topics**: (i) the dynamics of the water geochemistry, major ions
15 and trace elements; (ii) the stable water isotopes of precipitation and rivers; and (iii) the water uses by
16 the inhabitants. **As in most mountain environments, the Khumbu area** is threatened by climate change,
17 which impacts the cryosphere and consequently the people and the landscapes. Moreover, changes in
18 water use are also related to new needs stemming from tourism, which strongly affect local livelihood.
19 For the first two topics, new results are presented. They provide details on the global chemical quality
20 of the river water and show how certain elements are seasonally influenced and how other elements
21 allow us to distinguish the water origins within the study zone. Beside the use of stable isotopes to
22 determine mainly the origin of the water flow in the rivers, the isotopic patterns confirm the double
23 climatic influence of the westerly fluxes in the winter season and of the Asian monsoon in the summer
24 season. **Regarding water use, the study confirms that the chemical quality of the water course is good,**
25 **but does not conclude on the biological quality, which has not been investigated.** In conclusion, we
26 attempt to predict the future of the geochemistry patterns submitted to the double pressure of climate
27 change and the surge in tourism.

28 **1 Introduction**

29 The future of the cryosphere (glacier and snow cover) in the Hindu Kush Himalaya high mountains is
30 a major concern (Pörtner et al. 2019; Wester et al. 2019); it is threatened not only by global warming
31 due to greenhouse gas emissions, but also by local air pollution due to the atmospheric brown cloud,
32 and especially the transportation and deposition of black carbon aerosol (Bonasoni et al. 2010; Kaspari
33 et al. 2011; Jacobi et al. 2015) from human activities in the densely inhabited regions of the south and
34 southwest of the central Himalaya mountain range as well as the rapid increase of tourist activity
35 (Jacquemet 2018).

36 In this context, the Paprika and Preshine projects (see Funding section) joined the efforts of Nepalese,
37 French, and Italian research teams (see Acknowledgments section) to explore the impact of these
38 anthropogenic constraints on the water cycle dynamics in the Dudh Koshi River Basin (**Figure 1**) on

39 the south side of Mount Everest (8847 m). Several reasons justified the choice of this study zone that
40 is characterized by two confluent watercourses, the Imja River and the Khumbu River, respectively,
41 originating from the southern and western faces of the main range of Mount Everest and its satellite
42 summits.

43 Among these reasons, the following are particularly important in the context of this article:

- 44 • Relative **facility** of access with the Everest Base Camp Trail;
- 45 • **Settlements at high altitude (above 3500 m) where inhabitants are facing a wide range of**
46 **changes beside climatic one as a more tourism-centered economy involving integration to**
47 **global markets, agropastoral and lifestyles changes, and new migration patterns (Puschiasis**
48 **2019);**
- 49 • Presence of a high-altitude scientific laboratory, the Pyramid of Lobuche (5050 m),
50 administrated by the Italian Ev-K2/CNR association in agreement with the Nepalese Academy
51 of Science and Technology (NAST).

52 In this framework, a working task of the Paprika and Preshine projects has been devoted to the
53 identification of water resources and the perception of this held by the local inhabitants. **In the**
54 **preliminary exchanges with the scientists of the Paprika and Preshine projects, the Khumbu valley**
55 **inhabitants manifested a deep concern regarding their water resource and its future. They were acutely**
56 **aware that climate and economic changes will have a direct impact on the environment in which they**
57 **live. As a consequence, it appears as a necessity to also aboard the climate processes and the water**
58 **balance through the geochemical angle, even though this was not the primary route chosen for these**
59 **projects.**

60 The village of Pangboche, which includes several settlements, was chosen as the most convenient. The
61 main settlement is located at an elevation of approx. 3950 m on the right bank of the Imja River, 4 km
62 after the confluence of its two main branches: the Khumbu River flowing from the north and the Upper
63 Imja River flowing from the west. An important concern of the local population is the future of the
64 water resources, not only in quantity, but also in quality. Considering the latter point, it was also stated
65 that the water quality could be a **substantial** indicator of the water flow processes, especially regarding
66 the different origins of these flows: glacier melt, **snowmelt, groundwater**, or direct surface flow.

67 During the past decade, geochemistry studies have been conducted of the Himalaya water flows (e.g.,
68 Jeelani et al. 2011; Ghezzi et al. 2017), but no study has been undertaken in the context of very high
69 altitudes covering dynamically an entire year. This issue underlines the exploratory character of the
70 current study, which, however, does not aim to address all the questions raised in this exceptional
71 framework.

72 Numerous isotopic precipitation and river studies have been carried out in Himalaya at the local or
73 regional scale in the past few years (Garziona et al. 2000; Wen et al. 2012; Jeelani et al. 2013; Balestrini
74 et al. 2014; Balestrini et al. 2016; He and Richards 2016; Ren et al. 2017; Florea et al. 2017; Jeelani
75 and Deshpande 2017; Jeelani et al. 2017; Guo et al. 2017; Li and Garziona 2017; Kumar et al. 2018;
76 Verma et al. 2018; Shen and Poulsen 2019; Singh et al. 2019). The main aim of these studies was to
77 link the isotopic variability recorded in precipitation to climate parameters and air mass circulation
78 and the transfer of this isotopic signal through the global and complex altitudinal hydrosystem from
79 glaciers to tropical valleys. Regional precipitation studies of the southern external border of Himalaya
80 (Jeelani and Deshpande 2017) from Kashmir (western Himalaya) to Assam (eastern Himalaya), or of
81 the whole Tibetan Plateau (Li and Garziona 2017), showed that the isotopic variation observed in
82 precipitation across the Himalayas conforms to the regional repartition of the two main moisture
83 sources: the westerly fluxes and Asian monsoon. Local studies of precipitation isotopes were carried

84 out in central Nepal, Kathmandu, and the north of Kathmandu (Wen et al. 2012) as well as in the
85 Khumbu Valley at the Pyramid Laboratory (Balestrini et al. 2014; Balestrini et al. 2016).

86 The current paper aims to present, analyze and discuss, on the one hand, the geochemical behavior of
87 the water flows used by the inhabitants of Pangboche for their activities, during the year 2011,
88 exploring the conductivity, pH, major ions, and trace elements dissolved in the water; and, on the other
89 hand, the water-stable isotopes in the precipitation and river flows of the Khumbu area, during the
90 period from November 2014 to May 2017. The paper aims to link these **data** to the water origins and
91 seasonal variability in the context of global change.

92 **2 Study area and methods**

93 **2.1 Study area**

94 The climate of the study area is dominated from June to September by monsoon dynamics (Wang
95 2006; Bookhagen and Burbank 2010; Immerzeel et al. 2010; Turner and Annamalai 2012), but winter
96 and pre-monsoon precipitations can occur from December to April due to the Western Disturbances,
97 which are part of the westerlies entry, originating from the Mediterranean region (Pisharoty and Desai
98 1956; Madhura et al. 2015).

99 Above 5000 m in general, and lower during the winter, satellite imagery shows that the snow cover
100 can be **wide**; however, the difficulty of monitoring snowfall in high mountains (Sevruk 1989; Tahir et
101 al. 2011) does not allow us to quantify precisely the volume of snowfall in the study area. Recent
102 studies have explored the spatial distribution of precipitation in this area (Savéan et al. 2015; Gong-
103 Saholiariliva et al. 2016; Eeckman et al. 2017; Mimeau et al. 2019). **They roughly show, beside a large
104 local heterogeneity mainly due to the steep relief, the valley orientation and the slope aspect, a positive
105 gradient with the altitude until a peak of annual precipitation between 2500 and 3200 m and a negative
106 one above.**

107 The geology of the southern area of Mount Everest has been detailed by Bortolami (1998) and by
108 Searle et al. (2003). **It is dominated by Precambrian-Early Paleozoic sillimanite gneisses in the high
109 faces, which alternate in some places with intrusive Miocene leucogranites. The highest zone (Everest,
110 Lhotse), above 6500 m, presents Ordovician shale series and limestone layers.** Except for those slopes
111 covered by glaciers or rock glaciers, the valley slopes and valley bottoms are mainly composed of
112 fluvio-glacial deposits and debris, with the presence of moraines of different levels and ages.
113 According to Bortolami (1998), the composition of the rocks leads to a low weathering and a low
114 impact on the chemical composition of the flows. The same author notes that the aquifers located in
115 the debris material have a high porosity. Their thicknesses are largely unknown. By contrast, the
116 fissured rocks, which constitute the bed rock, are generally impermeable. A few other studies are
117 devoted to groundwater storage in the Himalayas. Although their findings are not very helpful with
118 regard to the geological characteristics (Dongol et al. 2005; Jeelani 2008) or the scale of the approach
119 used (Andermann et al. 2012), **these studies highlight a notable contribution of snow and glacier melt
120 to groundwater.** Andermann et al. (2012) assess the storing capacity of the whole Dudh Koshi basin
121 (3700 km²) to be approx. 300 mm, i.e., less than 20% of the average annual discharge, which represents
122 a low impact of the groundwater in our study area, considering that most of the reservoirs are very
123 likely concentrated in the bottom material of the middle and low elevations. Other authors, including
124 Nepal et al. (2014), Savéan et al. (2015), and Eeckman et al. (2019), consider in their modeling
125 approaches that the volume stored over a long period in groundwater reservoirs is **negligible**.

126 2.2 Water resources for local population

127 The Khumbu zone (Figure 1) encompasses an area of approximately 1100 km² along the border
128 between Nepal and the Tibet Autonomous Region of China. It is included in the Nepalese
129 administrative division of the Solu-Khumbu district. The area is divided into three major distinct
130 valleys—Imja Valley, Dudh Koshi Valley, and Bhote Koshi Valley—forming a U-shape, a testimonial
131 to the glacial erosion and draining of the main rivers in the region. The Dudh Koshi first meets the
132 Imja Khola on the eastern side of the region, and it then meets the Bhote Koshi before running out of
133 Khumbu toward the south into a deep gorge. Khumbu settlements span elevations from 2805 m
134 (Jorsalle) to 5170 m (Gorak Shep). The villages are located extensively on the rare alluvial terraces,
135 hanging valleys, and amphitheater slumps and comprise mostly south- and north-facing slopes.
136 Khumbu corresponds to the former Village Development Committees (VDCs, before administrative
137 restructuring in 2017) of Khumjung and Namche hosting approximately 3500 residents belonging
138 mostly to the Sherpa ethnic group with a growing number of non-Sherpa residents (Rais, Tamangs,
139 Magar, and Bahun-Chhetri). With the establishment of the Sagarmatha National Park (SNP) in 1976
140 and its designation as a UNESCO World Heritage Site in 1979, the economy of the region has shifted
141 to a more tourism-centered form (Spoon 2011). The number of visitors to the SNP increased to 45,000
142 in 2017 (Jacquemet 2018) leading to an important trekking and expedition tourism hub, including the
143 popular trekking route to Mount Everest Base Camp.

144 All these territorial and economic mutations have led to profound changes in water resources,
145 increasing needs previously limited to domestic (drinking water, cooking, personal hygiene),
146 agricultural (irrigation of barley), and religious purposes (water-driven prayer wheels, water spirit
147 shrine) (Aubriot et al. 2019). Water is taken directly from springs or small streams flowing through
148 the settlements or channeled by pipes to houses, since large rivers are not the primary source of water
149 for villagers (McDowell et al. 2012). In Pangboche village, changes appeared some 20 years ago with
150 the installation of running water supplying guest houses, a bottled-water manufacturing plant in 2003,
151 and a micro-hydroelectric plant in 2004 (Puschiasis 2015). Water has become a “commodity” (André-
152 Lamat 2017) with a proliferation of uses for tourism (shower, flushing toilets, bottled water) and for
153 electrification. Khumbu inhabitants have become highly dependent on reliable water supply systems
154 to respond to the new types of usages, which is key to local development. Nevertheless, there is a lack
155 of a proper management system at a regional level to reduce the pressure on water resources.

156 2.3 Methods of sampling and analysis

157 Labels A to Y refer to the sampling points shown in Figure 1 and described in Table 1. They are
158 ordered by altitude from bottom to top.

159 2.3.1 Conductivity, major and trace elements

160 Temperature, pH, and electrical conductivity ($T_{\text{ref}}=25^{\circ}\text{C}$) were measured in the field, using a portable
161 pH meter and conductivity meter (WTW 3210i®). Water samples (125 mL) were filtered in the field
162 with a PP syringe and Durapore® membrane (0.22 μm) and stored in acid-washed HDPE bottles.
163 Aliquots for major cations and trace elements were acidified with ultrapure HNO_3 (1% v/v). Samples
164 were stored at 4°C before reaching Montpellier for analysis.

165 Five sites in the surroundings of Pangboche village were selected for the water sampling (G, H, I, J,
166 L):

- 167 • The G point on the Imja River represents the reference site for the main river after the
168 confluence of the Khumbu branch and the Imja branch. These catchments include, on the one
169 hand, the large glaciers of the south side of the Everest Range and, on the other hand, the Imja

170 moraine lake, which concentrates the melting runoff from the majority of the glaciers of the
 171 upper Imja Valley.

- 172 • The Tauche point (J) on the east stream of the southern slope of the Tauche Peak (6542 m).
 173 This watercourse collects the melt flow from the very small glacier located on the peak summit.
- 174 • The Teouma (L) and Kisang (I) points on the central stream flow do not receive water of glacial
 175 origin. Because this watercourse flows through the village of Pangboche, the first point was
 176 chosen upstream and the second downstream from the village in order to analyze how the water
 177 quality of the stream is influenced by the village.
- 178 • The Chomar (H) source on the west side of Pangboche was also sampled, because its water
 179 was drawn and bottled in 2011 by a small company to be sold to tourists under the brand name
 180 of “*Namaste Sabina Tabuche Beiu.*” After 2013, the company no longer produced bottled water
 181 for unknown reasons.

182 The water flows were sampled 18 times between February and November 2011 following the complete
 183 annual cycle (Figure 2). A total of 12 samplings benefitted from a complete protocol (64 samples) and
 184 6 more samplings, in winter and autumn, from measurements of electrical conductivity and pH only.

185 Two complementary water samples were collected in June 2012 in Imja Lake (Y) and a rainfall
 186 reference was taken in the settlement of Pheriche (P). In addition, several measurements of electrical
 187 conductivity were carried out in different watercourses within the Imja River basin.

188 Chemical analyses were performed at the HydroSciences water chemistry laboratory in Montpellier
 189 (France). Total alkalinity was measured by acid titration with HCl 0.01 N (Gran method). Major ions
 190 (Cl^- , NO_3^- , SO_4^{2-} , Ca^{2+} , Mg^{2+} , Na^+ , and K^+) were analyzed by ionic chromatography (Dionex ICS
 191 1000®). The precision error was $< \pm 5\%$. Trace elements (Li, B, Al, Si, Ti, V, Cr, Mn, Fe, Co, Ni, Cu,
 192 Zn, As, Rb, Sr, Mo, Cd, Cs, Ba, Pb, and U) were analyzed with Q-ICPMS (X series2 Thermo
 193 Scientific®) on the AETE (*Analyse des Elements en Trace dans l'Environnement*) technical platform
 194 of Montpellier University. The precision error was $< \pm 8\%$.

195 2.3.2 Stable isotopes

196 Six sampling campaigns in rivers located between 1985 m (Kharikola, label A) and 5000 m (foot of
 197 glaciers, X, Y) were carried out (November to December 2014, November 2015, November 2016,
 198 March 2015, May 2016, May 2017).

199 In addition, during the study interval from November 2014 to December 2016, monthly rainfall was
 200 collected at Pangom (2890 m, E) using a homemade rain gauge with an 80-cm² cross-section in a 5-L
 201 plastic tank inside an isotherm box, which was linked to the gauge with a flexible pipe and hermetically
 202 sealed to avoid direct evaporation.

203 The rainfall and river samples were stored in amber glass bottles (25 mL) with conical plugs and
 204 transported in shaded conditions to the laboratory in Montpellier.

205 Water-stable isotopes were measured with an Isoprime® mass spectrometer on the LAMA platform
 206 of HydroSciences Montpellier (*Laboratoire Mutualisé d'Analyse des isotopes stables de l'eau*). The
 207 oxygen isotopic composition was measured after equilibration of 200 μL of water with CO_2 via the
 208 dual-inlet technique, with an overall precision of $\pm 0.06\%$. Deuterium was measured by continuous-
 209 flow using a Eurovector Pyr-OH® elemental analyzer converting 0.5- μL injections of water to H_2 on
 210 Cr powder at 1070°C, with an overall precision of $\pm 0.6\%$.

211 Water isotopic compositions are reported as $\delta^{18}\text{O}$ and $\delta^2\text{H}$ on the V-SMOW scale.

212 3 Results

213 3.1 Electrical conductivity and pH

214 **Figure 2 shows** the dynamics of the electrical conductivity and pH during the year 2011 at the five
215 measurement points (G, H, I, J, L) of the Pangboche area.

216 Regarding electrical conductivity, the absolute values are below 60 $\mu\text{S}/\text{cm}$. These very low values
217 indicate the slight level of mineralization of the flows. Specifically, the five sites present two main
218 behaviors: (i) Kisang and Teouma located on the same watercourse have an almost identical and
219 constant extremely low conductivity during the year (approx. 20 $\mu\text{S}/\text{cm}$), (ii) for Tauche and Imja the
220 values are 2–3 times higher, with a slight decrease during and shortly after the monsoon (July-
221 October), meaning that the increasing runoff generates a dilution effect. The Chomar site fits between
222 the two, with a decrease during the monsoon season.

223 The pH varies between 7 and 8, except for Pangboche-Chomar bottled drinking water (8.6) and for the
224 rain sample (6.8). The different sites present a short-term variability from date to date. However, two
225 main behaviors can be observed: (i) for the slope water courses (Tauche, Kisang, Teouma, and
226 Chomar), the amplitude of the short-term variability reaches 0.5 and a relative dilution effect appears
227 during the monsoon; (ii) the valley river (Imja) has an almost stable pH value (≈ 7.8) during the course
228 of the year, but higher than the pH of the slope water courses.

229 3.2 Major ions

230 **The following ranges in concentration were shown by the major cations and anions:** Ca^{2+} (1.1-11.1
231 mg/L), Mg^{2+} (0.1-0.7 mg/L), Na^+ (0.4-1.8 mg/L), K^+ (0.2-1.3 mg/L), HCO_3^- (5.1-32.3 mg/L), SO_4^{2-}
232 (0.4-14.5 mg/L), NO_3^- (0.1-1.5 mg/L), Cl^- (0.1-0.6 mg/L). **Silica ranges from 1.3 to 20.8 mg/L .** Average
233 concentrations of major ions are reported in Table 2. The Piper diagram for major cations and anions
234 (Figure 3 and Table 2) shows variations in the chemical composition of the surface waters, which is
235 dominated by Ca^{2+} and HCO_3^- . The waters are mainly of $\text{Ca}^+-\text{Mg}^+-\text{HCO}_3^-$ type. Waters influenced by
236 glacier melt (Tauche and Imja sites) exhibit an enrichment in SO_4^{2-} , particularly for the Tauche site
237 during the monsoon season. Ca^{2+} is the dominant cation contributing more than 70% to the cation
238 budget, followed by Na^+ (< 20%) and Mg^{2+} (<10%). In Kisang waters and to a less extent in Teouma
239 waters, before the monsoon season, Na^+ is the dominant cation. Cl^- and NO_3^- concentrations are very
240 low, <0.6 mg/L and <1.5 mg/L , respectively. The HCO_3^- contribution to the anion budget ranges
241 between 60 and 90%, except for Tauche water during the monsoon season, which evolves to a
242 $\text{Ca}^+-\text{Mg}^+-\text{SO}_4^{2-}$ type. The origin of sulfates is found in sulfide oxidation via glacier runoff, as suggested
243 by Hodson et al. (2002), because no anhydrite or gypsum have been identified in the region. The plot
244 of $\text{Ca}^++\text{Mg}^++\text{Na}^+$ versus $\text{HCO}_3^-+\text{SO}_4^{2-}$ from all the waters shows that most of the samples lie close to
245 the 1:1 line, indicating the dissolution of calcite, dolomite, silicates, and sulfides (Figure 4) **as**
246 **suggested by Crespo et al. (2017).**

247 For all major elements, including SiO_2 , the temporal evolution of the concentrations displays a dilution
248 effect during the monsoon season, except for the Imja site where an increase in the concentration of all the
249 major elements occurs during the same season, especially in August 2011, which corresponds to the
250 maximum glacier melt. This enrichment demonstrates that the glaciated catchment undergoes more intense
251 **chemical weathering taking place beneath the glacier** than catchments that do not have a glacier **because**
252 **the CO_2 dissolved in the proglacial zone with the aerated flow conditions characteristic of the meltwater**
253 **environments may promote chemical weathering by maintaining the acid potential of the water (Reynold**
254 **& Johnson 1972) in Singh and Hasnain (1998).**

255 3.3 Trace elements

256 Average concentrations for measured trace elements are presented in Table 3. Dissolved trace elements
 257 such as Li, B, Ni, Zn, Cu, Rb, Sr, Ba, and U show a dilution effect during the monsoon season at the
 258 Teouma, Kisang, Tauche, and Chomar sites whereas the Imja site in the same season exhibits, except
 259 for boron, a high concentration increase, by a factor of 10 to 100, as shown, for example, for rubidium
 260 (Figure 5). The origin of this increase can be found in the glacier melt enriched in subglacial material
 261 leached by the heavy rain during the monsoon. This phenomenon underlines the integrating power of
 262 the Imja Khola River. On the other hand, Al, Ti, Fe, and Mn to a lesser extent increase in all the sites
 263 during the monsoon season. In comparison with the Upper Mustang rivers in the western region of
 264 Nepal Himalaya (Ghezzi et al. 2017), the concentrations are elevated, from 5 to 6600 µg/L for Al, from
 265 0.5 to 485 µg/L for Ti, from 5 to 7130 µg/L for Fe, and from 2 to 200 µg/L for Mn. These elements
 266 are mobilized by the surface runoff during the monsoon season and their common origin is to be found
 267 in the weathered bedrock.

268 In regards of the WHO drinking water guidelines, no major or trace elements exceed the recommended
 269 values, even if the concentrations for some major or trace elements of the Imja River are elevated.

270 3.4 Stable isotopes

271 Three complete years (2014–2016) of meteorological data (P, T) are available at the Pangom station
 272 (2885 m, label D) (Chevallier et al. 2017), and a monthly sampling of rainfall for water isotope analysis
 273 was carried out between November 2014 and December 2016. The comparison of all the results is only
 274 qualitative owing to the small temporal record at the Pangom weather station.

275 The mean annual temperature measured at Pangom in 2015 was 6.7°C (7.6°C in 2014 and 8.0°C in
 276 2016) with lower temperatures in the dry season (min. in December: -1.1°C) and higher temperatures
 277 during the monsoon season (Figure 6) (max. in June: 12°C). In the higher part of the Khumbu valley
 278 at the Pyramid Laboratory station, monthly temperatures follow the same pattern ranging between -12
 279 and 4°C for the 2012–2014 interval (Balestrini et al. 2016).

280 3.4.1 Precipitations

281 Annual rainfall in Pangom was 3046 mm in 2015 (3683 mm in 2014 and 3947 mm in 2016). The South
 282 Asia monsoon (JJAS) accounts for more than 80% of the precipitation amount (Figure 6) (84.7 to
 283 86.1% from 2014 to 2016) with no specific rainier month in this season (JAS between 888 and
 284 1075 mm).

285 During the sampling interval (November 2014 to December 2016, with a gap in May 2016), a large
 286 isotopic variation is observed (Figure 6): 3.25 to -15.26‰ V-SMOW for $\delta^{18}\text{O}$ and 43.3 to -109.5‰
 287 V-SMOW for $\delta^2\text{H}$. Figure 6 shows the isotopic composition of all precipitations giving a local water
 288 line following the equation:

$$289 \quad \delta^2\text{H} = 8.57 \delta^{18}\text{O} + 20.5 \quad (R^2 = 0.997; n = 25)$$

290 The slope is slightly higher than the slope of the global meteoric water line (GMWL,
 291 $\delta^2\text{H} = 8.13 \delta^{18}\text{O} + 10.13$) defined by Rozanski et al. (1993) and also shows an intercept $d = 20.5$ higher,
 292 close to the meteoric line of the precipitation in the southern Tibetan plateau (Yao et al. 2013):

$$293 \quad \delta^2\text{H} = 8.89 \delta^{18}\text{O} + 23.0 \quad (R^2 = 0.980; n = 374).$$

294 At the Pyramid Laboratory station at the weekly scale between June 2012 and December 2013,
 295 Balestrini et al. (2016) found:

$$296 \quad \delta^2\text{H} = 8.17 \delta^{18}\text{O} + 16.6$$

297 In Pangom, if one distinguishes between the seasons, the equations are:

298	ONDJFMAM (non-monsoon)	$\delta^2\text{H} = 8.46 \delta^{18}\text{O} + 20.6$	$(R^2 = 0.997; n = 17)$
299	JJAS (monsoon),	$\delta^2\text{H} = 8.52 \delta^{18}\text{O} + 18.4$	$(R^2 = 0.999; n = 8).$

300 The more enriched monthly values above -1‰ in $\delta^{18}\text{O}$ ($n=5$) do not show an evaporation mark; a high
301 deuterium excess is observed (between 17.4 and 21.6‰) for low to medium rainfall amount (21 to 142
302 mm). These values belong to the extra-monsoon season and are linked to **notable** continental recycling
303 mainly from non-fractional processes such as transpiration or soil evaporation. In the regional study
304 by Jeelani and Deshpande (2017), stations in Nepal and Assam also showed a high d-excess ($> 20\text{‰}$)
305 associated with a high $\delta^{18}\text{O} > -1\text{‰}$ value, suggesting a dominant influence of transpiration, increasing
306 the $\delta^{18}\text{O}$ of vapor over the forest floor (Lai and Ehleringer 2010).

307 The isotopic values recorded during the 2 years, including monsoon and extra-monsoon seasons,
308 display different patterns, globally more depleted in the monsoon season (2015, -10.05‰ ;
309 2016, -8.48‰ , weighted mean for $\delta^{18}\text{O}$) and more enriched in the extra-monsoon season
310 (2015, -4.48‰ ; 2016, -0.81‰ , weighted mean for $\delta^{18}\text{O}$). The much more enriched values in the extra-
311 monsoon season in 2016 could be an effect on isotope composition and deuterium excess in the
312 beginning of the monsoon season with a possibly late isotope re-equilibration of the air mass, perhaps
313 due to **higher** mixing with the recycled continental vapor. Indeed, in June and July 2016, isotope values
314 were more enriched than in June and July 2015, also with a greater d-excess. Then, it is only in August
315 2016, in the middle of the monsoon season, that isotope values and d-excess seem to be consistent with
316 isotope values in the monsoon season, and this continues until the beginning of the extra-monsoon
317 season (October 2016) with a dephasing of 2 months.

318 **The relationship between isotope values and temperature (temperature effect) shows an inverse**
319 **correlation with a low coefficient ($R = -0.336$; $n = 25$) as well as with rainfall (amount effect) with**
320 **$R = -0.392$, which are not significant using a t-distribution with $n-2$ degrees of freedom at a**
321 **significance level $\alpha = 0.05$; the critical values associated with $df = 23$ are ± 0.396 (Bravais-Pearson**
322 **table). The monsoon season corresponds to a more depleted rainfall (Dansgaard 1964). In fact, the**
323 **main effect on isotope variability in our site is the origin of air masses, as shown in previous regional**
324 **studies cited in this article or in the local Khumbu Valley at the Pyramid Laboratory (Balestrini et al.**
325 **2016).**

326 The year 2015, which is complete, gives a weighted annual value ($\Sigma(P_i \delta_i) / \Sigma P_i$) of -9.24‰ V-SMOW
327 for $\delta^{18}\text{O}$ and -60.1‰ V-SMOW for $\delta^2\text{H}$ (2016: 95.9‰ of rainfall, -8.20‰ and -50.6‰), which is in
328 good agreement with the altitude effect in the region, regarding the results obtained in Kathmandu
329 (1320 m, -8.7‰) and Nyalang (3811 m, -11.3‰) (Wen et al. 2012; Balestrini et al. 2016); at the
330 Pyramid Laboratory station (5050 m), the isotope content during the monsoon season in 2012 and 2013
331 does not show a large variation (-17.74 to -17.81‰ in $\delta^{18}\text{O}$). The gradient is $-0.23\text{‰} / 100$ m, in good
332 agreement with the range of the isotope altitudinal gradient in Himalaya (-0.15 , -0.33‰) (Wen et al.
333 2012).

334 The d-excess is a good indicator for evaluating the contribution of different water vapor sources (Clark
335 and Fritz 1997). In Himalaya, low d-excess values characterize moisture coming from the Indian
336 Ocean and the Bay of Bengal, and high values continental moisture carried by the Western Disturbance
337 (Jeelani and Deshpande 2017). At Pangom in 2015 and 2016, d-excess values during the monsoon
338 season were between 11.3 and 18.7‰ ($n = 8$, mean = 13.6‰), while in the two extra-monsoon seasons
339 (2015 and 2016) d-excess values were between 14.3 and 23.9‰ ($n = 14$, mean = 19.1‰).

340 At the Pyramid Laboratory, we have the same pattern for isotope content and d-excess during the
 341 monsoon (depleted values up to -30‰ for $\delta^{18}\text{O}$ and d-excess < 15‰) and the extra-monsoon seasons
 342 (more enriched values and high d-excess until 26‰). The difference observed with the local meteoric
 343 line (LML) in d-excess is due to the different repartition of measurements in the monsoon season
 344 (n = 38) and the extra-monsoon season (n = 8).

345 We note in the total observed interval a good correlation between oxygen-18 and d-excess values
 346 ($R^2 = 0.62$; n=25), which reaches $R^2 = 0.72$ if the more enriched point is removed (April 2016); this
 347 may indicate a slight alteration in isotope air mass signal by the evaporation process.

348 To conclude, in Pangom as in other Himalayan sites, the change in air circulation patterns, marine
 349 vapor from the Indian Ocean and the Bay of Bengal, on the one hand, and continental vapor from the
 350 Western Disturbances, on the other, modify the isotope composition and d-excess of precipitation.

351 3.4.2 Rivers

352 For the river isotope sampling, in the general spatial pattern, depleted values are observed in the
 353 headwaters of the streams and enriched values at lower elevations of the catchments. The water isotope
 354 variability of stream water shows a lower variability with respect to local precipitation at Pangom, in
 355 spite of altitudinal sampling (1981–4935 m) and six campaigns between November 2014 and May
 356 2017 (local sampling between one and six campaigns) that ranged from -10.10 to -18.39‰ for $\delta^{18}\text{O}$
 357 and from -64.5 to -135.8‰ for $\delta^2\text{H}$ (Figure 7, Table 4). The sampling was carried out at the beginning
 358 of the extra-monsoon season, with possibly the influence of the end of the monsoon season, and at the
 359 end of the extra-monsoon season. However, the variability registered is mainly very low, lower than
 360 0.6‰ for $\delta^{18}\text{O}$ for 89% of local stations. Two stations with at least five samplings (D – Pangom and J
 361 – Tauche) show a large difference; both stations in March 2015 have a high depleted value (-16.65 and
 362 -16.53‰ in $\delta^{18}\text{O}$, respectively); not considering this result, Pangom has a mean value of -10.47‰ with
 363 a range interval of 0.45 (n = 4) and Tauche has a mean value of -15.31‰ with a range interval of 1.22
 364 (n = 5). Both sampling points are located in non-glaciated catchment for Pangom and small glaciated
 365 catchment (**less than 1% of the basin area**) for Tauche. The river in this extra-monsoon season with
 366 few precipitations (at Pangom in 2015, precipitation amounts are **19 mm in January, 19 mm in**
 367 **February and 66 mm in March**) is supplied mainly by superficial aquifer whose main characteristic is
 368 an isotopic composition relatively constant over the year at a local altitudinal point (Jeelani et al. 2018).
 369 The main hypothesis to explain this important change is the presence of snow cover at higher altitude
 370 with more depleted isotopic content during this season, which was melting and supplied by direct
 371 runoff from the river.

372 Although there were no measurements during the monsoon season in this study, the works of
 373 Balestrini, Polesello, and Sacchi (2014) in the high part of the Khumbu Valley (> 4200 m) have shown
 374 a higher variability (2‰) close to glacier and morainic lake inflow and low variability (0.39‰ in $\delta^{18}\text{O}$)
 375 at Pheriche (label P in Figure 1) during monthly sampling between July and October 2008. The authors
 376 suggest that the area extension of the hydrological basin buffers the isotopic signal. Another fact is the
 377 difficulty to link directly the isotope content of monthly precipitation and isotopic content of river
 378 water at the same time.

379 The isotopic composition of the stream water in the whole study interval is close to the local
 380 precipitation regression line (Figure 7) following the equation:

$$381 \quad \delta^2\text{H} = 8.23 \delta^{18}\text{O} + 15.0 \quad (R^2 = 0.987; n = 58)$$

382 For each season the slope and the d-excess value can differ greatly, but the number of samples is small
383 (except for May 2017, which is close to the global river equation) and these variations are **not**
384 **representative** of a particular process:

385	November 2014	$\delta^2\text{H} = 8.11 \delta^{18}\text{O} + 4.1$	$(R^2 = 0.972; n = 5)$
386	March 2015	$\delta^2\text{H} = 7.56 \delta^{18}\text{O} + 22.2$	$(R^2 = 0.999; n = 9)$
387	November 2015	$\delta^2\text{H} = 6.71 \delta^{18}\text{O} + 9.3$	$(R^2 = 0.934; n = 11)$
388	May 2016	$\delta^2\text{H} = 8.24 \delta^{18}\text{O} + 16.3$	$(R^2 = 0.994; n = 10)$
389	November 2016	$\delta^2\text{H} = 8.08 \delta^{18}\text{O} + 13.3$	$(R^2 = 0.992; n = 9)$
390	May 2017	$\delta^2\text{H} = 8.47 \delta^{18}\text{O} + 19.1$	$(R^2 = 0.997; n = 17)$

391 The mean d-excess value at each sampling point is between 5.6 and 14.4‰. For the whole dataset,
392 d-excess values vary between 3.1 and 15.6‰ with 19% of samples lower than 10‰, which are altered
393 by an evaporation process. The samples with d-excess between 10 and 14‰ do not show a special
394 trend, likely linked to glacier melt and aquifer discharge where the main accumulation and recharge
395 are during monsoon season when the d-excess value of the monthly precipitation is between 11 and
396 14‰. For d-excess values higher than 14‰, there is possibly a partial contribution of rainfall or melted
397 snow during the extra-monsoon season where d-excess values of monthly precipitation can reach 24‰
398 during the 2014–2016 interval.

399 Contrary to the results of another study in southern Himalaya by Wen et al. (2012), who found a very
400 good correlation between the isotope content in the Boqu River and altitude ($n = 39$, $R^2 = 0.90$, Sept.
401 2011) between 1845 and 5060 m, the relationship between the altitude of the sampling sites and isotope
402 content is not well correlated ($R^2 = 0.399$; $n=18$) very likely due to the heterogeneity of the catchments
403 and their glacier cover varying between 0% and 70%. The river in catchments with glacier cover at all
404 altitudes is mainly controlled by the ice melting and by higher depleted value with respect to no glacier
405 catchments. This is the case of the Phakding samples, located at a low altitude (2620 m), which show
406 an isotope content in $\delta^{18}\text{O}$ of -15.89‰, with a 20.9% glacier cover (Everest catchment). By
407 comparison, the weighted mean annual rainfall in Pangom (2890 m) yields -9.24‰, in better
408 accordance with the isotope values collected in the Pangom River (watershed without glacier) and
409 reflecting the isotope composition of rainfall in the whole study area (-11.71‰).

410 By contrast, rivers in catchments without any or with small glacier cover (Kharikola, Pangom, Tauche,
411 Chomar, Teouma), spring (Lobuche spring), or surface flow not connected to glacier melt such as wet
412 saturated pastures (*kharka* in Nepali; e.g., Phulung Kharka) show (Figure 8) a better correlation with
413 altitude ($R^2 = 0.809$; $n = 8$). Focusing only on the river sampling points that depending on glacier melt,
414 the correlation with altitude is significantly improved ($R^2 = 0.525$; $n = 10$). Indirectly, the lower the
415 altitude, the more the glacier component in the river decreases and the more the aquifer component
416 increases.

417 The isotopic altitude gradient for river sampling in no or in a lightly glaciated catchments shows for
418 $\delta^{18}\text{O}$ a value of -0.20‰/100m; this is in the range (-0.11/- 0.36‰/100 m) of other studies referenced
419 by Wen et al. (2012) and Ren et al. (2017) in Himalaya and is close to results found by Florea et al.
420 (2017), in the same zone, i.e., -0.28‰/100 m. By comparison with the study of Florea et al. (2017), in
421 the Dudh Koshi River with a sampling set located between Gorak Shek (5180 m), upstream of
422 Lobuche, and downstream of Phakding (2550 m) in May 2011, values in $\delta^{18}\text{O}$ are between -17.9 and
423 -9.7‰. The relationship between $\delta^{18}\text{O}$ and $\delta^2\text{H}$ demonstrates a lower slope and d-excess value than
424 our global study, with the equation:

$$425 \quad \delta^2\text{H} = 7.8 \delta^{18}\text{O} + 4.0 \quad (R^2 = 0.94; n = 32)$$

426 Individually, tributary streams and direct sampling in the Dudh Koshi River show a d-excess ranging
 427 between 4.4‰ and 12.7‰ (72% of samples lower than 10‰), which is globally lower than the
 428 d-excess measured in this study. The slope is lower than 8, but overall the low d-excess values imply
 429 that an evaporation process during the study interval (Florea et al. 2017) may be due to the sampling
 430 time (end of extra-monsoon season), with warmer conditions than during the sampling times of this
 431 study.

432 **4 Discussion**

433 **4.1 Water origins**

434 Not surprisingly, the isotope properties of the precipitation highlight the double climatic influence
 435 from the arrival of the westerlies in winter and from the Asian monsoon in summer.

436 The isotope response to ground ice melt has been investigated since the mid-1970s (Stuiver et al.,
 437 1976; Fujino and Kato, 1978) who relies on isotope fractionation that occurs during phase changes
 438 (i.e. freezing, condensation, adsorption) and the resulting difference in the slope of the regression of
 439 δD on $\delta^{18}O$ with a slope between 3 and 7 (Jouzel and Souchez, 1982; Lacelle et al., 2011). Ala-aho et
 440 al. (2018) show in western Siberia the possible discrimination of water origin between precipitation,
 441 river, lakes and thawing permafrost. The slope of the regression of δD on $\delta^{18}O$ was lower than the
 442 precipitation (7.6) with soils/permafrost (4.64) < lakes (5.54) < rivers (6.08) and a strong variability
 443 of median isotope content in precipitation (-15.6‰ in $\delta^{18}O$), rivers (-15.3‰), soils/permafrost
 444 (-13.0‰) and lakes (-11.1‰) > rivers (-15.1‰). In our study case the river points do not show an
 445 obvious influence of thawing permafrost during the sampling period which correspond before or after
 446 monsoon when temperatures are lower, may-be during monsoon period of higher temperature, an
 447 important thawing permafrost could be detected in some rivers.

448 Locally, the results of the current study confirm that few chemical patterns can be used to distinguish
 449 the waterflow origins during the different seasons. Rb, as Li, Cu, Sr, Ba and SiO₂, originating from the
 450 minerals of the bedrock, characterizes substantially the water originating from glacier melt, as shown
 451 in Figure 5, especially during the monsoon season. Nevertheless, the isotopic results appear to be less
 452 useful for that task, even if differences are observed: The isotopic climate signal in the water courses
 453 is very likely mixed with the signal emitted by the storage in groundwater temporary reservoirs, which
 454 limits a clear interpretation. Factually, it depends on the sampling location and of the ratio of
 455 glacierized area. In the high altitudes (> 4000 m) the river reflects the isotope content mainly of the
 456 ice and snow melt because the climatic conditions do not allow an important weathering of the rocks
 457 and a strong development of an aquifer structure; the consequence is a reduced groundwater capacity,
 458 and a fast groundwater circulation reflecting isotope content of ice and snow. At lower altitude, the
 459 weathering is higher and the aquifer can develop itself with a higher storage capacity involving local
 460 recharge by rainfall; the isotope content is enriched with respect to ice and snow melt (altitude effect):
 461 the lower the altitude, the richer is the isotope content of total flow. It is a consequence of the higher
 462 base flow in the dry season and of the higher contribution of the surface runoff in the monsoon season,
 463 this last being enriched in isotope with respect to ice and snow melt more depleted.

464 However, the meltwater marking (glacier as snow cover melt) by the isotopes can be more visible than
 465 by the chemical signature in downstream sampling sites, because it is less dissolved, with the
 466 inconvenience of a smoothed seasonal effect. The result at the Phakding (20.9‰ glacier covered) and
 467 Pangom (no glacier) stations, detailed in the previous section, is, therefore, significant.

468 The pH remains in a relatively narrow range in the different sampling points and does not seem useful
 469 for characterizing the water paths or the seasons, while electrical conductivity shows slightly higher

470 values for flows originating from glaciers and lower values in the monsoon runoffs of streams not fed
471 by glacier melt (Figure 2).

472 In addition to the previous considerations, complementary observations on electrical conductivity were
473 made in the main rivers of this area and in the Imja Lake during a 3-day interval in the second half of
474 June 2012, in the early monsoon season. They are summarized in Table 5, which shows that the flows
475 arising from the Imja Lake are approximately twofold less mineralized than those of the Khumbu upper
476 valley. Both basins have similar areas and ratios of glaciated surfaces. Because the flows are from the
477 same geological and glaciological origin, the conductivity difference observed can only be explained
478 by the presence of the lake. The higher value observed in the lateral Imja River, which does not flow
479 from the lake, confirms this hypothesis. This phenomenon could be attributed to the sedimentation
480 only within the lake of the solid load generated by the glacier abrasion, due to quieter hydraulic
481 conditions. This hypothesis is reinforced by the visual observations at the confluence between the Imja
482 and the Khumbu rivers, which showed that the turbulence of the runoff was higher in the Khumbu
483 branch than in the Imja branch (Figure 9).

484 4.2 Water uses

485 Before commenting, it must be stressed that in the framework of this study no analysis was performed
486 regarding the bacterial quality of the water used by the inhabitants and by the visitors. The reason is
487 that, at the time of the study, the only laboratory for analyzing samples, poorly equipped and without
488 dedicated manpower, was located in the Khumjung Hospital, close to the village of Namche Bazar,
489 several hours' walking distance from the sampling points. This is unfortunate, because the sources of
490 bacterial pollution are numerous, especially high-altitude pastures, perfunctory toilet installations,
491 uncontrolled waste disposal, etc. (Manfredi et al. 2010). These sources of pollution are increasing with
492 the rapid development of tourist activities. Furthermore, inhabitants in Pangboche expressed more
493 concerns about the future of the water quality than about water quantity since no proper sewage system
494 exists and they are witnessing a dissemination of plastic waste in streams.

495 The quality of the natural water can be chemically considered good with a very low mineralization
496 degree. It appears that the reticence to consider the water of the large valley river is mainly justified
497 by the danger in accessing and harvesting it and also by its white color, due to the fine particles
498 mentioned in the previous section. This particular property gave its name to the Dudh Koshi River,
499 which means *Milk River* in Nepali. Nevertheless, these statements cannot conclude on the drinkability
500 of the river water, since, as written above, organic and microbiological analysis have not been done in
501 the current study framework.

502 The sampling points L (Pangboche-Teouma) and I (Pangboche-Kisang) were chosen for their location,
503 upstream and downstream of the village, respectively, in order to examine an eventual degradation due
504 to the human activities. No notable differences can be observed in terms of the major ions (Table 2).
505 Nevertheless, in Figure 4, the trace elements collected throughout the year in Teouma (upstream)
506 appear grouped, when a dispersion is noted for those collected downstream in Kisang. This dispersion
507 is very likely due to the limited pollution of the water used in the village. Shortly after Kisang, the
508 slope torrent is intercepted by the large Dudh Koshi River, where the low chemical pollution is
509 dissolved.

510 Finally, the issue of bottled water consumption by tourists is of some importance to the local economy,
511 because it is a non-negligible income for the communities (Puschiasis 2015; Jacquemet 2018). Several
512 small companies have been established in the region to exploit this niche. One of them collected water
513 at the Pangboche-Chomar point (labeled H in Figure 1) and, after a basic filtration process, bottled it.
514 The bottled water was also analyzed with the same procedure as the other samples, except that it was

515 transported to France after several months in the original PET bottle and not in a standard analysis
516 recipient (see Section 2.3.1). As shown in Figure 4, no difference is observed between the bottle and
517 the other samples from the Chomar site. In Table 2, a few differences are notable, especially regarding
518 pH, Cl⁻, NO₃⁻, and Na⁺. They can be explained by the very long storage in a bad-quality recipient, but
519 this is the reality for most of the water bottles available in the study zone. Nevertheless, in terms of
520 chemical quality, the bottled water and the river water are similar. It seems that for some reason the
521 water company did not pursue the exploitation of the Chomar site, which no longer functioned after
522 2013. However, water bottles from other places, particularly those collected in the surroundings of
523 Namche Bazar, were sold in the Pangboche shops and lodges.

524 **5 Conclusion**

525 **Between many studies, the recent IPCC special report on the cryosphere future (Pörtner et al. 2019)**
526 **confirms the loss of cryospheric mass and the rapid permafrost thaw. It is also verified in the Central**
527 **Himalaya, which presents threats on physical entities (water resources, flood, landslide, avalanche)**
528 **and on ecosystems (forest, tundra). The Khumbu inhabitants are strongly preoccupied by this situation,**
529 **which directly impacts their livelihood. In addition, they** face difficulties in terms of inequalities in the
530 social water management system, failing to regulate proper access of water in villages (Puschiasis
531 2015; Faulon and Sacareau 2020). More than climatic variations, changes in water use over the past
532 decades are due to a growing need for tourism and for domestic purposes. Regarding the future of
533 accessible water resources, this does not seem to be threatened in terms of quantity, even if seasonal
534 pressures should lead to a better water management, especially during the high season of tourism
535 activities (Aubriot et al. 2019). However, water quality could evolve in a worrisome direction.

536 Apart from the bacteriological issue, which is not considered here, the points addressed could change
537 as follows:

- 538 • The isotopic signature of precipitation and rivers is a good indicator of climate change and flow
539 paths. It should be periodically analyzed. On the one hand, it could follow changes observed
540 in the seasonal precipitation patterns in the study region (Shea et al. 2015). On the other hand,
541 it facilitates the recognition of the transitory storage of surface water (glacier, snow cover, or
542 underground reservoirs).
- 543 • In this study the chemical properties of the water used for domestic activities do not seem to
544 be hazardous to human and animal health at present. However, with changes in precipitation
545 and river regimes, in land use and land cover due to economic income, in cropping strategies,
546 in the very low level of waste and toilet water management, the current fragile balance could
547 be seriously jeopardized. The project of road construction in the valley, for instance, validated
548 until Surkhe, close to Lukla (“The Rising Nepal: Everest Region Closer with Bridge over
549 Sunkoshi” 2020), will lead to the importation of chemical products and molecules that have
550 been thus far unknown.

551 **6 Conflict of Interest**

552 The authors declare that the research was conducted in the absence of any commercial or financial
553 relationships that could be construed as a potential conflict of interest.

554 **7 Author Contributions**

555 Pierre Chevallier coordinated the whole study, including the field collection, wrote the introduction,
556 discussion, and conclusion sections, and assembled the different parts of the paper. Jean-Luc Seidel
557 contributed to the geochemistry analysis of the major ions and trace elements and Jean-Denis Taupin
558 of the stable isotopes. Ornella Puschiasis lived in Pangboche during the whole year in 2011 at an

559 elevation of 4000 m, collecting the water samples and she wrote the parts regarding water use by the
560 local inhabitants.

561 **8 Funding**

562 The global research action, the sample analysis, and the PhD grant, followed by a post-doctoral grant,
563 of Ornella Puschiasis were supported by *Agence Nationale de la Recherche - France* (references:
564 ANR-09-CEP-005-04/PAPRIKA and ANR-13-SENV-005-03/PRESHINE). Some monitoring
565 equipment was acquired through the *Glacioclim SNO* (French National Observation Service).

566 **9 Acknowledgments**

567 The analyses of major ions and trace elements were done by Sandra Van Exter and Jean-Luc Seidel,
568 and the analysis of stable isotopes by Nicolas Patris at the *Laboratoire HydroSciences Montpellier*
569 (*CNRS, IRD, University of Montpellier*). Dawa Nuru Sherpa translated the dialogs with Pangboche's
570 inhabitants and facilitated the measurements. Ang Jangmu Sherpa collected and stored the
571 precipitation samples in Pangom. Yves Arnaud, Olivia Aubriot, Anneke De Rouw, François Delclaux,
572 Judith Eeckman, Michel Esteves, Frédéric Hernandez, Devesh Koirala, Luc Neppel, Rémi Muller,
573 Marie Savéan, Joëlle Smadja, and Patrick Wagnon participated in the field operations, **as well as**
574 **extraordinary, indispensable and friendly local porters.**

575 Yves Arnaud and Isabelle Sacareau were, respectively, the coordinators of the Paprika and Preshine
576 projects, which benefited from a partnership with the following institutions: Nepalese Academy of
577 Science and Technology (Kathmandu, Nepal), EvK2-CNR Association (Bergamo, Italy), International
578 Center of Integrated Mountain Development (Kathmandu, Nepal), Tribhuvan University (Kathmandu,
579 Nepal), and Department of Hydrology and Meteorology (Kathmandu, Nepal).

580 **Finally, the authors thank the two anonymous reviewers who allow to substantially improve the**
581 **definitive version of the paper.**

582 **10 References**

- 583 **Ala-aho, P., C. Soulsby, O.S. Pokrovsky, S.N. Kirpotin, J. Karlsson, S. Serikova, S.N. Vorobyev, R.M.**
584 **Manasyopov, S. Loiko and D. Tetzlaff, 2018. "Using stable isotopes to assess surface water**
585 **source dynamics and hydrological connectivity in a high-latitude wetland and permafrost**
586 **influenced landscape". *Journal of Hydrology* 556 (2018) 279–293**
- 587 Andermann, C., L. Longuevergne, S. Bonnet, A. Crave, P. Davy, and R. Gloaguen. 2012. "Impact of
588 Transient Groundwater Storage on the Discharge of Himalayan Rivers." *Nature Geoscience* 5:
589 127–32. <https://doi.org/10.1038/ngeo1356>.
- 590 André-Lamat, Véronique. 2017. "De l'eau Source à l'eau Ressource : Production d'un Capital
591 Environnemental Ou d'un Commun. L'exemple de l'eau Domestique Au Pharak (Népal)."
592 *Développement Durable et Territoires*. <https://halshs.archives-ouvertes.fr/halshs-01959313>.
- 593 Aubriot, Olivia, Marie Faulon, Isabelle Sacareau, Ornella Puschiasis, Etienne Jacquemet, Joëlle
594 Smadja, Véronique André-Lamat, Céline Abadia, and Alix Muller. 2019. "Reconfiguration of
595 the Water–Energy–Food Nexus in the Everest Tourist Region of Solukhumbu, Nepal."
596 *Mountain Research and Development* 39 (1). <https://doi.org/10.1659/MRD-JOURNAL-D-17-00080.1>.
- 598 Balestrini, Raffaella, Carlo A. Delconte, Elisa Sacchi, Alana M. Wilson, Mark W. Williams, Paolo
599 Cristofanelli, and Davide Putero. 2016. "Wet Deposition at the Base of Mt Everest: Seasonal
600 Evolution of the Chemistry and Isotopic Composition." *Atmospheric Environment, Acid Rain*

- 601 and its Environmental Effects: Recent Scientific Advances Papers from the Ninth International
 602 Conference on Acid Deposition, 146 (December): 100–112.
 603 <https://doi.org/10.1016/j.atmosenv.2016.08.056>.
- 604 Balestrini, Raffaella, Stefano Polesello, and Elisa Sacchi. 2014. “Chemistry and Isotopic Composition
 605 of Precipitation and Surface Waters in Khumbu Valley (Nepal Himalaya): N Dynamics of High
 606 Elevation Basins.” *Science of The Total Environment* 485–486 (July): 681–92.
 607 <https://doi.org/10.1016/j.scitotenv.2014.03.096>.
- 608 Bonasoni, P., P. Laj, A. Marinoni, M. Sprenger, F. Angelini, J. Arduini, U. Bonafe, et al. 2010.
 609 “Atmospheric Brown Clouds in the Himalayas: First Two Years of Continuous Observations
 610 at the Nepal Climate Observatory-Pyramid (5079 m).” *Atmospheric Chemistry and Physics* 10:
 611 7515–31. <https://doi.org/10.5194/acp-10-7515-2010>.
- 612 Bookhagen, Bodo, and D. W. Burbank. 2010. “Toward a Complete Himalayan Hydrological Budget:
 613 Spatiotemporal Distribution of Snowmelt and Rainfall and Their Impact on River Discharge.”
 614 *Journal of Geophysical Research-Earth Surface* 115. <https://doi.org/10.1029/2009jf001426>.
- 615 Bortolami, Giancarlo. 1998. “Geology of the Khumbu Region, Mt Everest, Nepal.” In *Limnology of*
 616 *High Altitude Lakes in the Mt Everest Region, Nepal*, edited by A. Lami and G Giussani, 57:41–
 617 49. Memorie Dell’ Istituto Italiano Di Idrobiologia.
- 618 Chevallier, Pierre, François Delclaux, Patrick Wagnon, Luc Neppel, Yves Arnaud, Michel Esteves,
 619 Devesh Koirala, et al. 2017. “Paprika - Preshine Hydrology Data Sets in the Everest Region
 620 (Nepal). 2010-18.” Data base. 2017. <https://doi.org/10.23708/000521>.
- 621 Clark, Ian, and Peter Fritz. 1997. *Environmental Isotopes in Hydrogeology*. Boca Raton, New York:
 622 Lewis Publisher.
- 623 **Crespo, S., J. Aranibar, L. Gomez, M. Schwikowski, S. Bruetsch, L. Cara and R. Villalba, R. 2017.**
 624 **Ionic and stable isotope chemistry as indicators of water sources to the Upper Mendoza River**
 625 **basin, Central Andes of Argentina. *Hydrological Sciences Journal*, 62(4), 588-605. doi:**
 626 **10.1080/02626667.2016.1252840**
- 627 Dansgaard, W. 1964. “Stable Isotopes in Precipitation.” *Tellus*, no. 16: 436–68.
 628 <https://doi.org/10.1111/j.2153-3490.1964.tb00181.x>.
- 629 Dongol, B. S., J. Merz, M. Schaffner, G. Nakarmi, P. B. Shah, S. K. Shrestha, P. M. Dangol, and M.
 630 P. Dhakal. 2005. “Shallow Groundwater in a Middle Mountain Catchment of Nepal: Quantity
 631 and Quality Issues.” *Environmental Geology* 49 (December): 219–29.
 632 <https://doi.org/10.1007/s00254-005-0064-5>.
- 633 Eeckman, J., P. Chevallier, A. Boone, L. Neppel, A. De Rouw, F. Delclaux, and D. Koirala. 2017.
 634 “Providing a Non-Deterministic Representation of Spatial Variability of Precipitation in the
 635 Everest Region.” *Hydrol. Earth Syst. Sci.* 21 (9): 4879–93. <https://doi.org/10.5194/hess-21-4879-2017>.
- 637 Eeckman, Judith, Santosh Nepal, Pierre Chevallier, Gauthier Camensuli, Francois Delclaux, Aaron
 638 Boone, and Anneke De Rouw. 2019. “Comparing the ISBA and J2000 Approaches for Surface
 639 Flows Modelling at the Local Scale in the Everest Region.” *Journal of Hydrology* 569
 640 (February): 705–19. <https://doi.org/10.1016/j.jhydrol.2018.12.022>.
- 641 Faulon, Marie, and Isabelle Sacareau. 2020. “Tourisme, gestion sociale de l’eau et changement
 642 climatique dans un territoire de haute altitude : le massif de l’Everest au Népal.” *Journal of*
 643 *Alpine Research | Revue de géographie alpine*, no. 108–1 (April).
 644 <https://doi.org/10.4000/rga.6759>.

- 645 Florea, Lee, Broxton Bird, Jamie K. Lau, Lixin Wang, Yanbin Lei, Tandong Yao, and Lonnie G.
 646 Thompson. 2017. “Stable Isotopes of River Water and Groundwater along Altitudinal
 647 Gradients in the High Himalayas and the Eastern Nyainqentanghla Mountains.” *Journal of*
 648 *Hydrology: Regional Studies* 14 (December): 37–48.
 649 <https://doi.org/10.1016/j.ejrh.2017.10.003>.
- 650 Fujino K. and K. Kato. 1978. “Determination of oxygen isotopic concentration in the ground ice of a
 651 tundra area”. In “Joint Studies on Physical and Biological Environments in the Permafrost,
 652 Alaska and North Canada, July to August 1977”, Kinoshita S. (ed). The Institute of Low
 653 Temperature Science, Hokkaido University: Sapporo; 77–83.
- 654 Garzzone, C.N., J. Quade, P.G. De Celles, and N.B. English. 2000. “Predicting Paleoelevation of Tibet
 655 and the Himalaya from $\Delta 18\text{O}$ vs Altitude Gradients in Meteoric Water across the Nepal
 656 Himalaya.” *Earth Planet Sci. Lett.*, no. 183: 215–29.
- 657 Ghezzi, L., R. Petrini, C. Montomoli, R. Carosi, K. Paudyal, and R. Cidu. 2017. “Findings on Water
 658 Quality in Upper Mustang (Nepal) from a Preliminary Geochemical and Geological Survey.”
 659 *Environmental Earth Sciences* 76 (19): 651. <https://doi.org/10.1007/s12665-017-6991-0>.
- 660 Gongga-Saholiariliva, N., L. Neppel, Pierre Chevallier, F. Delclaux, and M. Savéan. 2016.
 661 “Geostatistical Estimation of Daily Monsoon Precipitation at Fine Spatial Scale: Koshi River
 662 Basin.” *Journal of Hydrologic Engineering*, April, 05016017.
 663 [https://doi.org/10.1061/\(ASCE\)HE.1943-5584.0001388](https://doi.org/10.1061/(ASCE)HE.1943-5584.0001388).
- 664 Guo, Xiaoyu, Lide Tian, Rong Wen, Wusheng Yu, and Dongmei Qu. 2017. “Controls of Precipitation
 665 $\Delta 18\text{O}$ on the Northwestern Tibetan Plateau: A Case Study at Ngari Station.” *Atmospheric*
 666 *Research* 189 (June): 141–51. <https://doi.org/10.1016/j.atmosres.2017.02.004>.
- 667 He, Siyuan, and Keith Richards. 2016. “Stable Isotopes in Monsoon Precipitation and Water Vapour
 668 in Nagqu, Tibet, and Their Implications for Monsoon Moisture.” *Journal of Hydrology* 540
 669 (September): 615–22. <https://doi.org/10.1016/j.jhydrol.2016.06.046>.
- 670 Hodson, Andy, Phil Porter, Andy Lowe, and Paul Mumford. 2002. “Chemical Denudation and Silicate
 671 Weathering in Himalayan Glacier Basins: Batura Glacier, Pakistan.” *Journal of Hydrology* 262
 672 (1): 193–208. [https://doi.org/10.1016/S0022-1694\(02\)00036-7](https://doi.org/10.1016/S0022-1694(02)00036-7).
- 673 Immerzeel, W.W., L. P. H. van Beek, and M. F. P. Bierkens. 2010. “Climate Change Will Affect the
 674 Asian Water Towers.” *Science* 328: 1382–85. <https://doi.org/10.1126/science.1183188>.
- 675 Jacobi, H.-W., S. Lim, M. Ménégoz, P. Ginot, P. Laj, P. Bonasoni, P. Stocchi, A. Marinoni and Y.
 676 Arnaud. 2015. “Black carbon in snow in the upper Himalayan Khumbu Valley, Nepal:
 677 observations and modeling of the impact on snow albedo, melting, and radiative forcing”. *The*
 678 *Cryosphere* 9, 1685–1699. <https://doi.org/10.5194/tc-9-1685-2015>
- 679 Jacquemet, Etienne. 2018. “The Sherpa Community in the ‘Yak Donald’s’ Era : Locational Struggles
 680 for Access to Resources in Mount Everest Touristic Region (Nepal).” Theses, Université
 681 Michel de Montaigne - Bordeaux III. <https://tel.archives-ouvertes.fr/tel-02275425>.
- 682 Jeelani, Ghulam. 2008. “Aquifer Response to Regional Climate Variability in a Part of Kashmir
 683 Himalaya in India.” *Hydrogeology Journal* 16 (December): 1625–33.
 684 <https://doi.org/10.1007/s10040-008-0335-9>.
- 685 Jeelani, Ghulam, N. A. Bhat, K. Shivanna, and M. Y. Bhat. 2011. “Geochemical Characterization of
 686 Surface Water and Spring Water in SE Kashmir Valley, Western Himalaya: Implications to
 687 Water-Rock Interaction.” *Journal of Earth System Science* 120 (October): 921–32.

- 688 Jeelani, Ghulam, and R. D. Deshpande. 2017. "Isotope Fingerprinting of Precipitation Associated with
689 Western Disturbances and Indian Summer Monsoons across the Himalayas." *Journal of Earth*
690 *System Science* 126 (8): 108. <https://doi.org/10.1007/s12040-017-0894-z>.
- 691 Jeelani, Ghulam, Rajendrakumar D. Deshpande, Rouf A. Shah, and Wasim Hassan. 2017. "Influence
692 of Southwest Monsoons in the Kashmir Valley, Western Himalayas." *Isotopes in*
693 *Environmental and Health Studies* 53 (4): 400–412.
694 <https://doi.org/10.1080/10256016.2016.1273224>.
- 695 Jeelani, Ghulam, U. Saravana Kumar, and Bhishm Kumar. 2013. "Variation of $\Delta^{18}\text{O}$ and ΔD in
696 Precipitation and Stream Waters across the Kashmir Himalaya (India) to Distinguish and
697 Estimate the Seasonal Sources of Stream Flow." *Journal of Hydrology* 481 (February): 157–
698 65. <https://doi.org/10.1016/j.jhydrol.2012.12.035>.
- 699 Jeelani, Ghulam, Rouf A. Shah and Rajendrakumar D. Deshpande. 2018. "Application of Water
700 Isotopes to Identify the Sources of Groundwater Recharge in a Karstified Landscape of Western
701 Himalaya". *Journal of Climate Change* 4(1):37-47.
- 702 Jouzel J. and R.A. Souchez. 1982. "Melting and refreezing at the glacier sole and the isotopic
703 composition of the ice". *Journal of Glaciology* 28: 35–42.
- 704 Kaspari, S. D., M. Schwikowski, M. Gysel, M. G. Flanner, S. Kang, S. Hou, and P. A. Mayewski.
705 2011. "Recent Increase in Black Carbon Concentrations from a Mt. Everest Ice Core Spanning
706 1860-2000 AD." *Geophysical Research Letters* 38 (February).
707 <https://doi.org/10.1029/2010gl046096>.
- 708 Kumar, Amit, Sameer K. Tiwari, Akshaya Verma, and Anil K. Gupta. 2018. "Tracing Isotopic
709 Signatures (ΔD and $\Delta^{18}\text{O}$) in Precipitation and Glacier Melt over Chorabari Glacier–
710 Hydroclimatic Inferences for the Upper Ganga Basin (UGB), Garhwal Himalaya." *Journal of*
711 *Hydrology: Regional Studies* 15 (February): 68–89. <https://doi.org/10.1016/j.ejrh.2017.11.009>.
- 712 Lacelle, D. 2011. "On the d^{18}O , dD and D -excess relations in meteoric precipitation and during
713 equilibrium freezing: theoretical approach and field examples". *Permafrost and Periglacial*
714 *Processes* 22, 13–25.
- 715 Lai, C.T., and J.R. Ehleringer. 2010. "Deuterium Excess Reveals Diurnal Sources of Water Vapor in
716 Forest Air." *Oecologia*. <https://doi.org/10.1007/s00442-010-1721-2>.
- 717 Li, Lin, and Carmala N. Garzzone. 2017. "Spatial Distribution and Controlling Factors of Stable
718 Isotopes in Meteoric Waters on the Tibetan Plateau: Implications for Paleoelevation
719 Reconstruction." *Earth and Planetary Science Letters* 460 (February): 302–14.
720 <https://doi.org/10.1016/j.epsl.2016.11.046>.
- 721 Madhura, R.K., R. Krishnan, J.V. Revadekar, M. Mujumdar, and B. N. Goswami. 2015. "Changes in
722 Western Disturbances over the Western Himalayas in a Warming Environment." *Climate*
723 *Dynamics*, no. 44: 1157–68.
- 724 Manfredi, Emanuela Chiara, Bastian Flury, Gaetano Viviano, Sudeep Thakuri, Sanjay Nath Khanal,
725 Pramod Kumar Jha, Ramesh Kumar Maskey, et al. 2010. "Solid Waste and Water Quality
726 Management Models for Sagarmatha National Park and Buffer Zone, Nepal Implementation
727 of a Participatory Modeling Framework." *Mountain Research and Development* 30 (2): 127–
728 42. <https://doi.org/10.1659/MRD-JOURNAL-D-10-00028.1>.
- 729 McDowell, G., J. D. Ford, B. Lehner, L. Berrang-Ford, and A. Sherpa. 2012. "Climate-Related
730 Hydrological Change and Human Vulnerability in Remote Mountain Regions: A Case Study

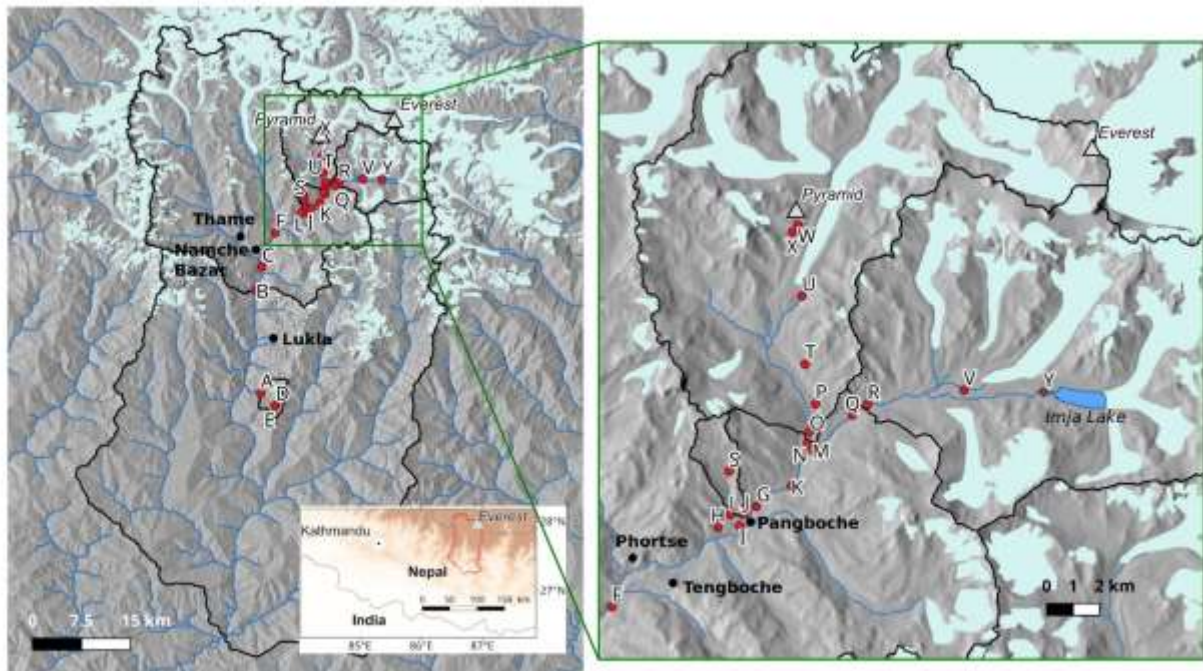
- 731 from Khumbu, Nepal.” *Regional Environmental Change*, July, 1–12.
732 <https://doi.org/10.1007/s10113-012-0333-2>.
- 733 Mimeau, Louise, Michel Esteves, Hans-Werner Jacobi, and Isabella Zin. 2019. “Evaluation of Gridded
734 and In Situ Precipitation Datasets on Modeled Glacio-Hydrologic Response of a Small
735 Glacierized Himalayan Catchment.” *Journal of Hydrometeorology* 20 (6): 1103–21.
736 <https://doi.org/10.1175/JHM-D-18-0157.1>.
- 737 Nepal, S., P. Krause, W.-A. Flügel, M. Fink, and C. Fischer. 2014. “Understanding the Hydrological
738 System Dynamics of a Glaciated Alpine Catchment in the Himalayan Region Using the J2000
739 Hydrological Model.” *Hydrological Processes* 28 (3): 1329–44.
740 <https://doi.org/10.1002/hyp.9627>.
- 741 Pisharoty, P.R., and B.N. Desai. 1956. “Western Disturbances and Indian Weather.” *Indian J.*
742 *Meteorol. Geophys.*, no. 8: 333–38.
- 743 Pörtner, H.-O., Roberts, D.C., Masson-Delmotte, Valérie, P. Zhai, Tignor, M., Poloczanska, E.,
744 Mintenbeck, K., et al. 2019. “IPCC Special Report on the Ocean and Cryosphere in a Changing
745 Climate.” Geneva, Switzerland: IPCC. <https://www.ipcc.ch/srocc/home/>.
- 746 Puschiasis, Ornella. 2015. “Des enjeux planétaires aux perceptions locales du changement climatique :
747 pratiques et discours au fil de l’eau chez les Sherpa de la vallée du Khumbu (Everest, Népal).”
748 Doctorat, Nanterre: Université Paris Ouest Nanterre La Défense.
- 749 ———. 2019. “Un vent de changements souffle sur l’Everest. Multiples facettes de la perception de
750 la météorologie et du climat chez les Sherpa.” *ethnographiques.org*.
751 <http://www.ethnographiques.org/2019/Puschiasis>.
- 752 Ren, Wei, Tandong Yao, Shiyu Xie, and You He. 2017. “Controls on the Stable Isotopes in
753 Precipitation and Surface Waters across the Southeastern Tibetan Plateau.” *Journal of*
754 *Hydrology* 545 (February): 276–87. <https://doi.org/10.1016/j.jhydrol.2016.12.034>.
- 755 **Reynolds, R.C. and N.M Johnson. 1972. Chemical weathering in temperate glacial environment of the**
756 **Northern Cascade Mountains. *Geochim. Cosmochim. Acta* 36, 537-54.**
- 757 Rozanski, K., L. Araguas-Araguas, and R. Gonfiantini. 1993. “Isotopic Patterns in Modern Global
758 Precipitation.” In *Climate Change in Continental Isotopic Records*, 1–36. Geophysical
759 Monograph 78. American Geophysical Union.
- 760 Savéan, Marie, Francois Delclaux, Pierre Chevallier, Patrick Wagon, Nahossio Gongu-Saholiariliva,
761 Rajendra Sharma, Luc Neppel, and Yves Arnaud. 2015. “Water Budget on the Dudh Koshi
762 River (Nepal): Uncertainties on Precipitation.” *Journal of Hydrology* 531 (December): 850–
763 62. <https://doi.org/10.1016/j.jhydrol.2015.10.040>.
- 764 Searle, M. P., R. L. Simpson, R. D. Law, R. R. Parrish, and D. J. Waters. 2003. “The Structural
765 Geometry, Metamorphic and Magmatic Evolution of the Everest Massif, High Himalaya of
766 Nepal-South Tibet.” *Journal of the Geological Society* 160 (May): 345–66.
767 <https://doi.org/10.1144/0016-764902-126>.
- 768 Sevruck, B. 1989. “Reliability of Precipitation Measurements.” In *Not in File*, edited by B. Sevruck,
769 13–19. St Moriz, Switzerland: Swiss Federal Institute of Technology, Zürich.
- 770 Shea, J. M., P. Wagon, W. W. Immerzeel, R. Biron, F. Brun, and F. Pellicciotti. 2015. “A
771 Comparative High-Altitude Meteorological Analysis from Three Catchments in the Nepalese
772 Himalaya.” *International Journal of Water Resources Development* 31 (2): 174–200.
773 <https://doi.org/10.1080/07900627.2015.1020417>.

- 774 Shen, Hong, and Christopher J. Poulsen. 2019. “Precipitation $\delta^{18}\text{O}$ on the Himalaya–Tibet Orogeny
775 and Its Relationship to Surface Elevation.” *Climate of the Past* 15 (1): 169–87.
776 <https://doi.org/10.5194/cp-15-169-2019>.
- 777 Singh, Ajit T., Waliur Rahaman, Parmanand Sharma, C. M. Laluraj, Lavkush K. Patel, Bhanu Pratap,
778 Vinay Kumar Gaddam, and Meloth Thamban. 2019. “Moisture Sources for Precipitation and
779 Hydrograph Components of the Sutri Dhaka Glacier Basin, Western Himalayas.” *Water* 11
780 (11): 2242. <https://doi.org/10.3390/w11112242>.
- 781 Singh, Kumar Abhay, and Syed Iqbal Hasnain. 1998. “Major Ion Chemistry and Weathering Control
782 in a High Altitude Basin: Alaknanda River, Garhwal Himalaya, India.” *Hydrological Sciences*
783 *Journal* 43: 825–43. DOI: [10.1080/02626669809492181](https://doi.org/10.1080/02626669809492181)
- 784 Spoon, Jeremy. 2011. “The Heterogeneity of Khumbu Sherpa Ecological Knowledge and
785 Understanding in Sagarmatha (Mount Everest) National Park and Buffer Zone, Nepal.” *Human*
786 *Ecology* 39 (October): 657–72. <https://doi.org/10.1007/s10745-011-9424-9>.
- 787 **Stuiver, M. and I.C. Yang. 2020. “Everest Region Closer with Bridge over Sunkoshi”. January 16,**
788 **2020. <http://therisingnepal.org.np/news/1084>.**
- 789 Turner, Andrew G., and H. Annamalai. 2012. “Climate Change and the South Asian Summer
790 Monsoon.” *Nature Clim. Change* 2: 587–95. <https://doi.org/10.1038/nclimate1495>.
- 791 Verma, Akshaya, Amit Kumar, Anil K. Gupta, Sameer K. Tiwari, Rakesh Bhambri, and Suneet
792 Naithani. 2018. “Hydroclimatic Significance of Stable Isotopes in Precipitation from Glaciers
793 of Garhwal Himalaya, Upper Ganga Basin (UGB), India.” *Hydrological Processes* 32 (12):
794 1874–93. <https://doi.org/10.1002/hyp.13128>.
- 795 Wang, Bin. 2006. *The Asian Monsoon*. Springer-Praxis Books in Environmental Sciences. Berlin,
796 Heidelberg, New York, Chichester: Springer, Praxis Publishing.
- 797 Wen, Rong, LiDe Tian, YongBiao Weng, ZhongFang Liu, and ZhongPing Zhao. 2012. “The Altitude
798 Effect of $\Delta^{18}\text{O}$ in Precipitation and River Water in the Southern Himalayas.” *Chinese Science*
799 *Bulletin* 57 (14): 1693–98. <https://doi.org/10.1007/s11434-012-4992-7>.
- 800 Wester, Philippus, Arabinda Mishra, Aditi Mukherji, and Arun Bhakta Shrestha, eds. 2019. *The Hindu*
801 *Kush Himalaya Assessment. Mountains, Climate Change, Sustainability and People*. ICIMOD.
802 Kathmandu, Nepal: Springer Nature. <https://doi.org/10.1007/978-3-319-92288-1>.
- 803 Yao, Tandong, Valerie Masson-Delmotte, Jing Gao, Wusheng Yu, Xiaoxin Yang, Camille Risi,
804 Christophe Sturm, et al. 2013. “A Review of Climatic Controls on $\Delta^{18}\text{O}$ in Precipitation over
805 the Tibetan Plateau: Observations and Simulations.” *Reviews of Geophysics* 51 (4): 525–48.
806 <https://doi.org/10.1002/rog.20023>.
807

808

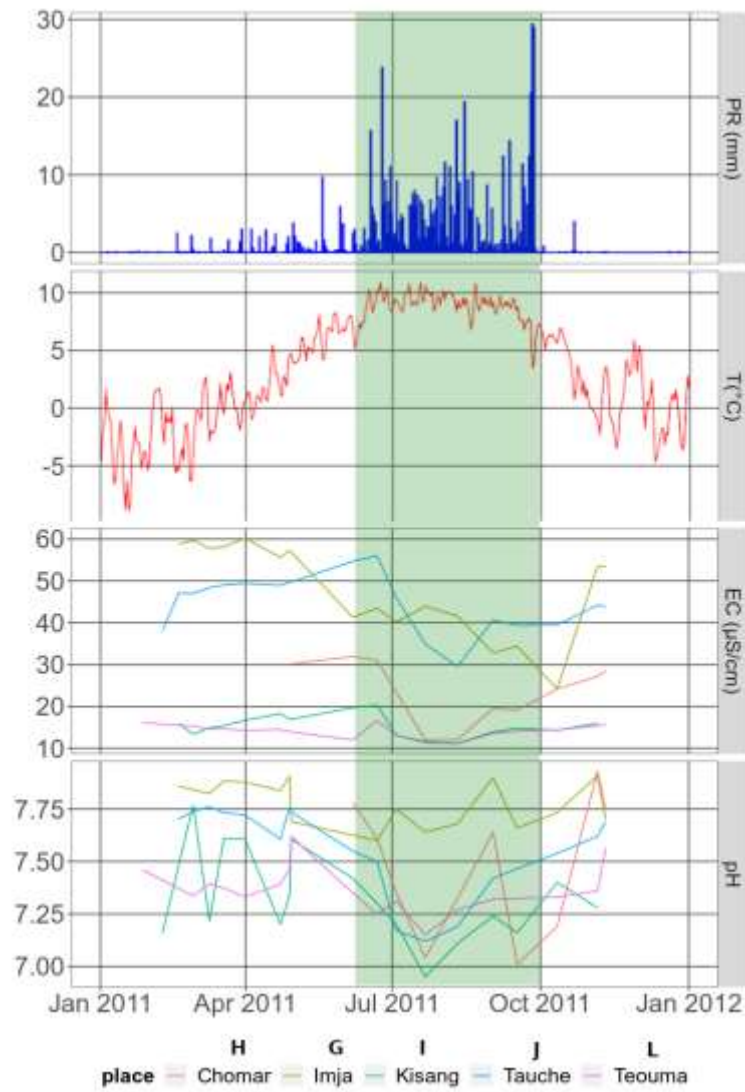
809 **11 Figures and tables**

810 **11.1 Figures**



811

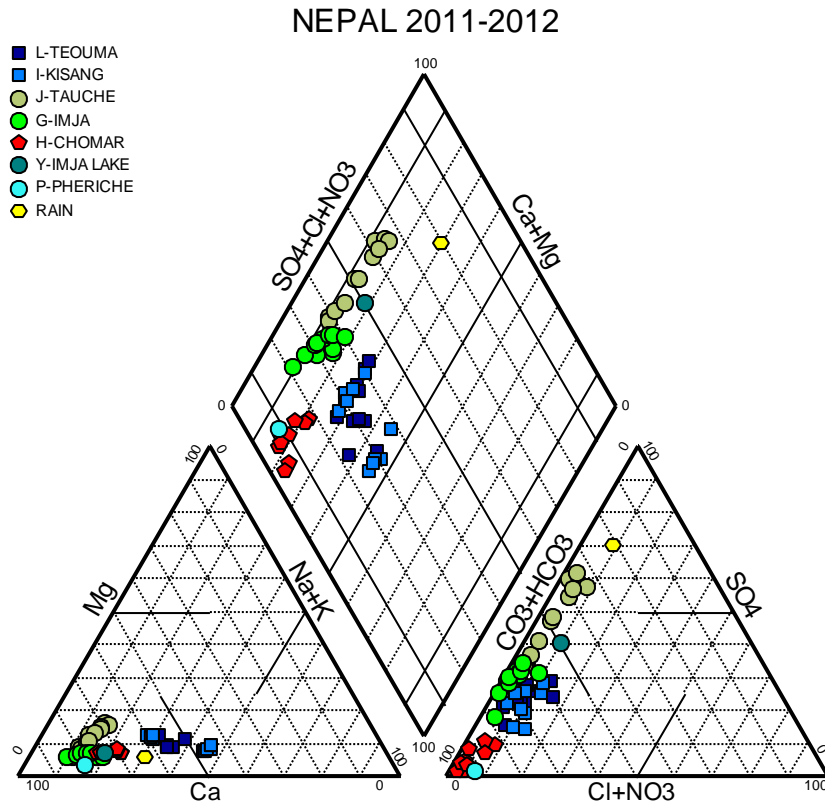
812 **Figure 1.** Bottom left: location of the Dudh Koshi River basin (red line). Left: Dudh Koshi River basin and sub-
813 basins, southern Mount Everest. Right: details of the Upper Khumbu and Imja area. The red dots represent
814 the sampling points. The labels refer to Table 1. Sources: for relief, digital elevation model based on Spot-
815 HRS images with a 40-m resolution (Gardelle et al. 2013); for glacier extension, Randolph Glacier Inventory
816 (RGI Consortium 2017).



817

818 **Figure 2.** Year 2011: Daily precipitation (PR) and temperature (T) data at Pangboche weather station vs.
 819 electrical conductivity (EC) and pH at the five sampling points around Pangboche (~4000 m). The monsoon
 820 season (JJAS) is highlighted in green.

821



822

823

Figure 3. Piper diagram of the major ions in the collected samples.

824

825

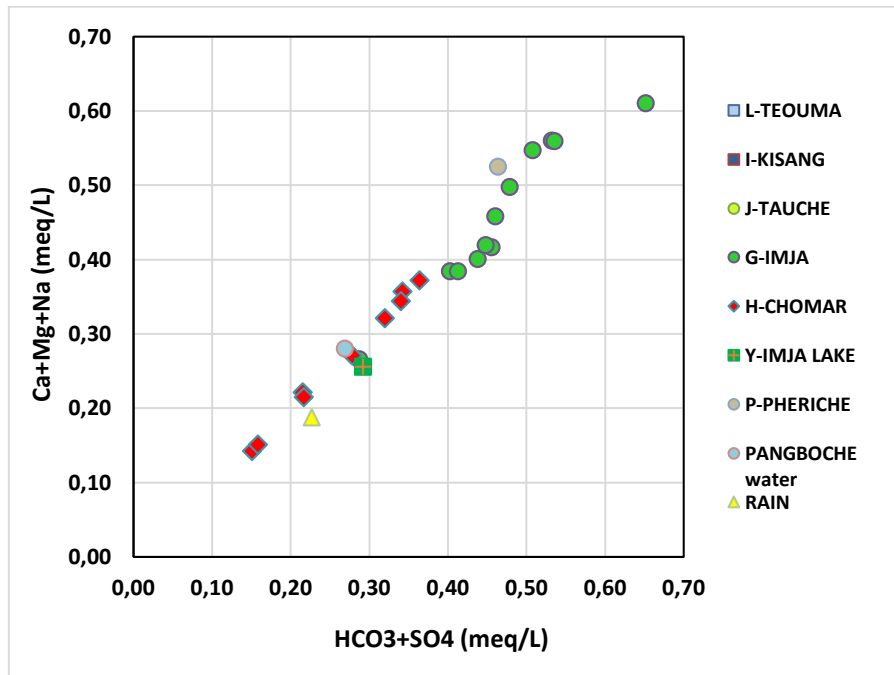


Figure 4. Ca+Mg+Na versus HCO₃+SO₄ (meq/L)

826

827

828

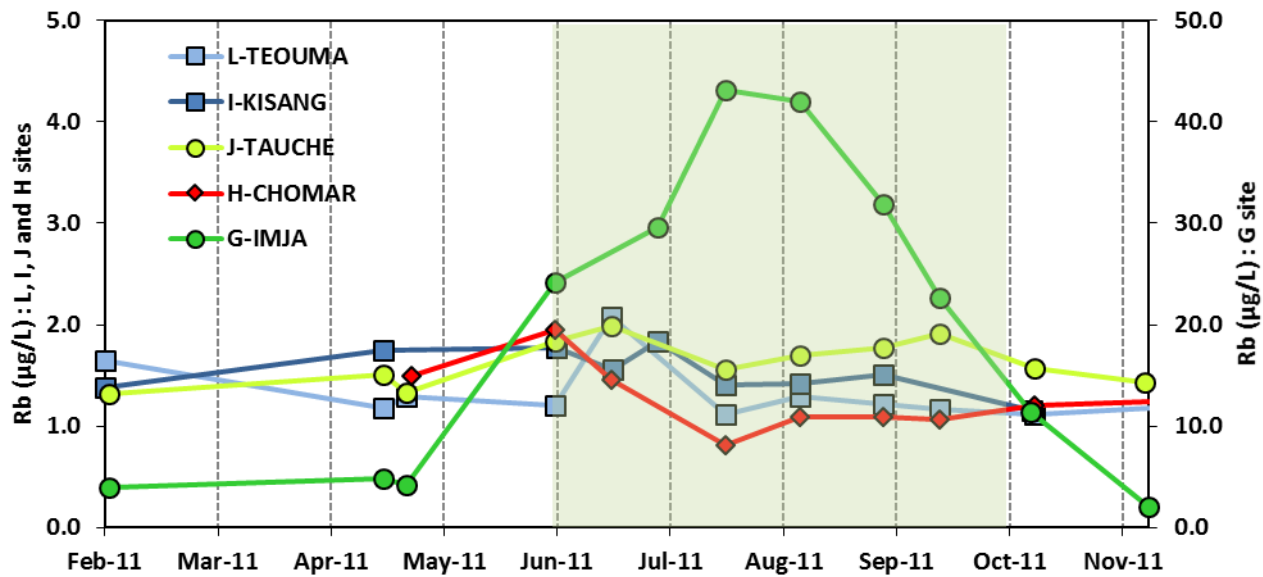


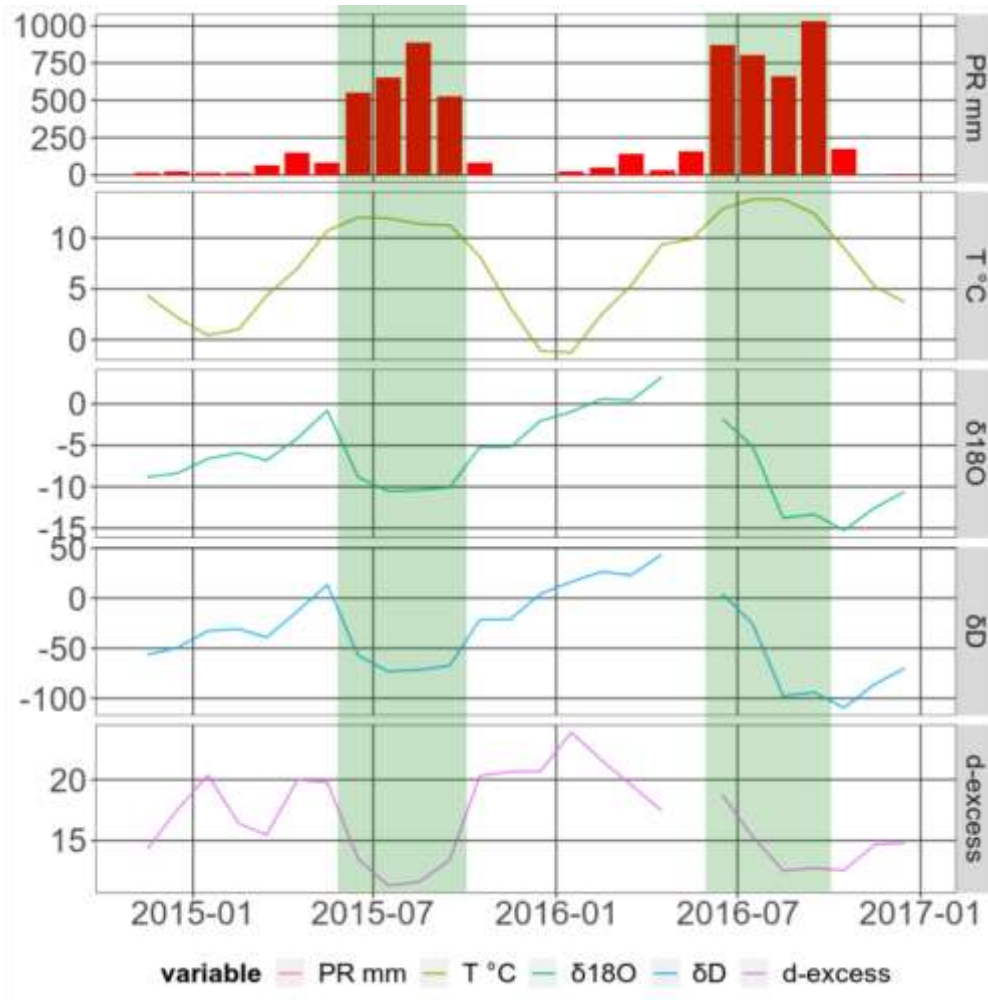
Figure 5. Temporal variation of Rb concentration. The monsoon season is highlighted in green.

829

830

831

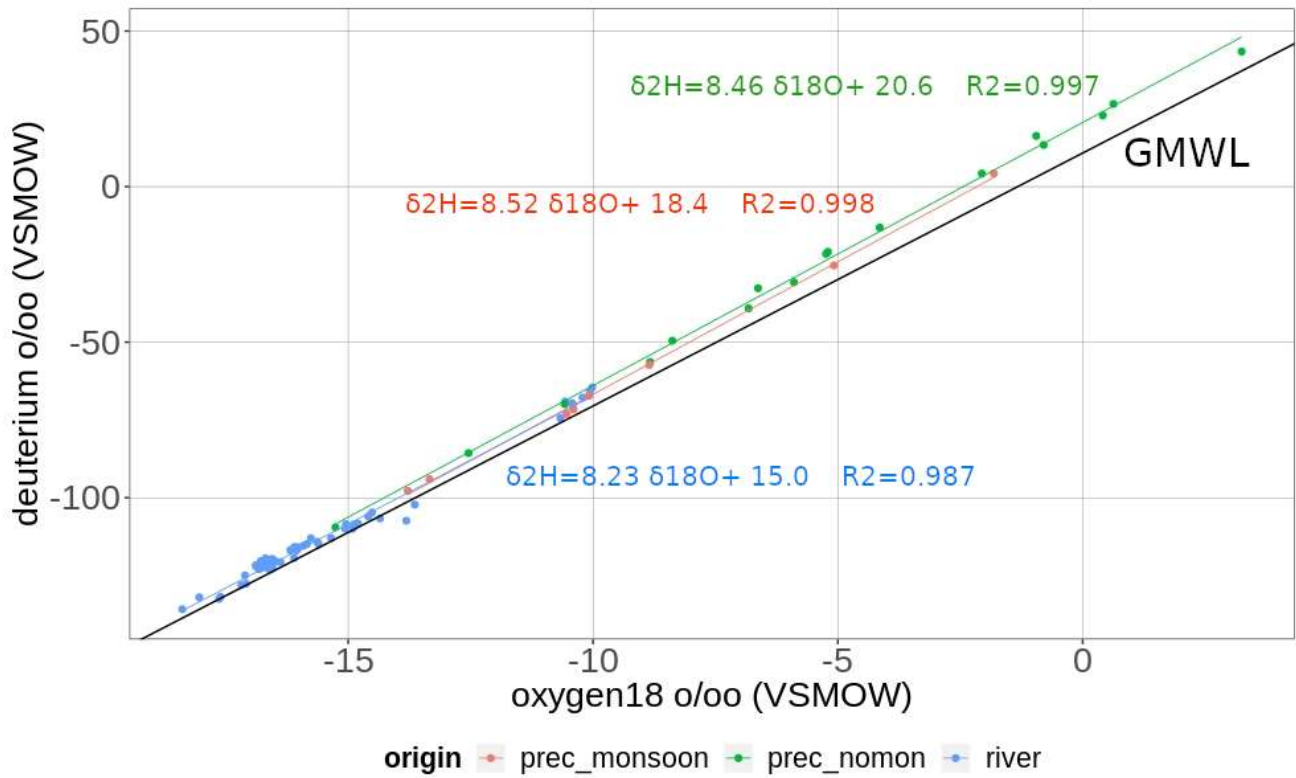
832



833

834 Figure 6: Monthly precipitation data in Pangom (E): precipitation (PR), air temperature (T), and stable isotopes
 835 ($\delta^{18}\text{O}$, δD , D-excess, ‰ VSMOW). The monsoon seasons (JJAS) are highlighted in green.

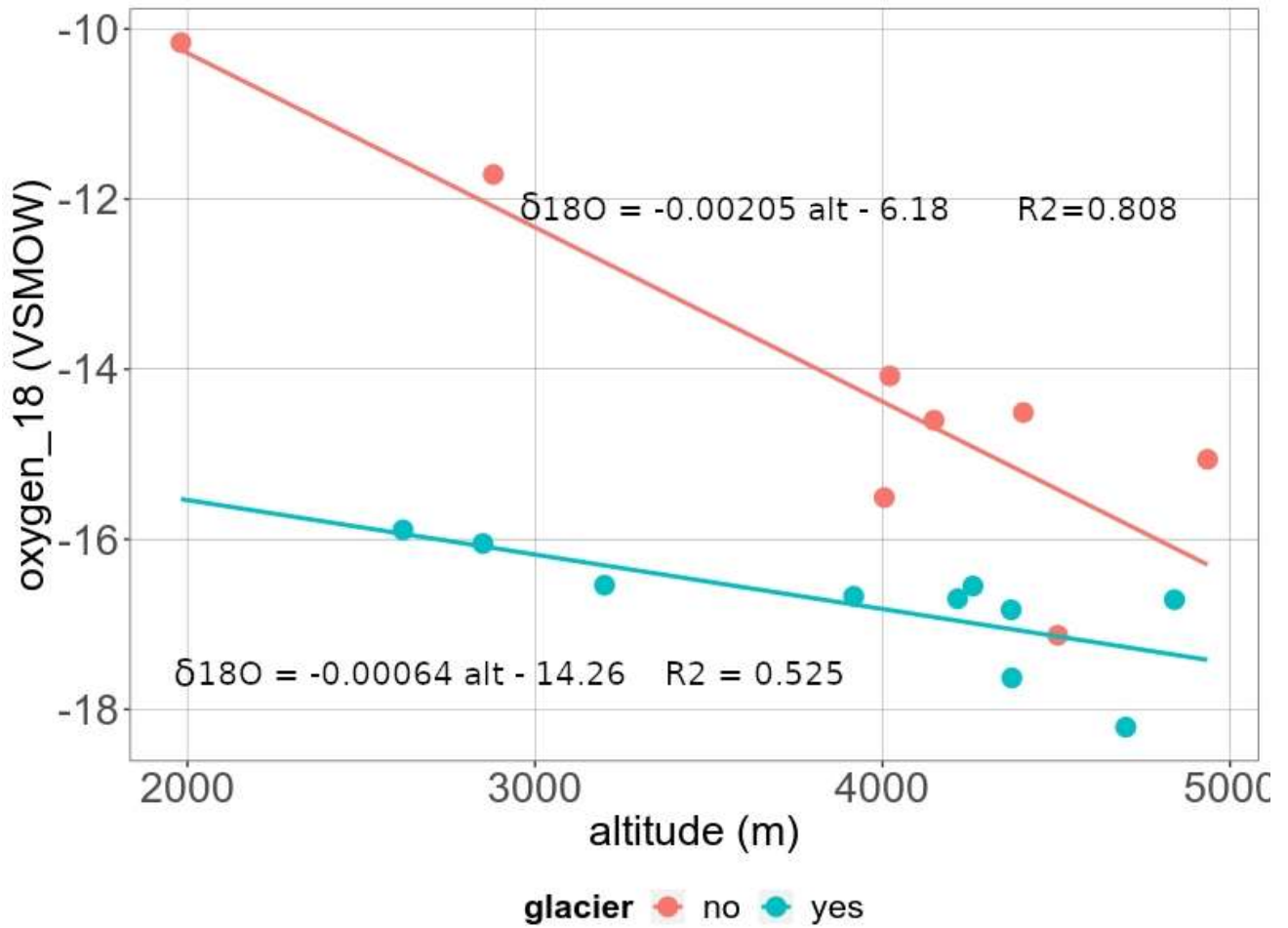
836



837

838 Figure 7: $\delta^{18}\text{O}$ vs $\delta^2\text{H}$ for precipitation samples in Pangom (monsoon and extra-monsoon seasons in red and
 839 green, respectively) and for river samples in blue, compared with the Global Meteoric Water Line (GMWL)

840



841

842

843

844

Figure 8: Isotope altitude gradient from sampling in no glacier watershed (isotope value determined by local rainfall and aquifer isotope value), and sampling in partial glacier watershed (isotope value determined by mixing between melt from high altitude and local rainfall and aquifer isotope value).

845

846



847 Figure 9: Confluence of the Khumbu River (down left) and the Imja River branch (upper right). The image has
848 been saturated for a better depiction of the difference in turbidity between both branches. Picture by
849 P. Chevallier, 19 June 2012.

850

851 **11.2 Tables**

852 Table 1: Main characteristics of the sampling points (ordered by altitude)

Name (+)	Label (++)	Coordinates			Data type (*)	Sample (**)	Glaciers (***)
		Longitude	Latitude	Altitude (m)			
Kharikhola	A	86°43'16"	27°36'22"	1981	R	IS	N
Phakding	B	86°42'47"	27°44'53"	2620	R	IS	Y
Jorsalle	C	86°43'19"	27°46'48"	2850	R	IS	Y
Pangom river	D	86°44'38"	27°35'24"	2880	R	IS	N
Pangom village	E	86°44'35"	27°35'17"	2890	P	IS	-
Phuki Tenga	F	86°44'35"	27°49'37"	3200	R	IS	Y
Pangboche-Imja	G	86°47'53"	27°51'40"	3917	R	MT IS	Y
Pangboche-Chomar	H	86°46'59"	27°51'14"	3930	R & bottle	MT	N
Pangboche-Kisang	I	86°47'31"	27°51'18"	3971	R	MT	N
Pangboche-Tauche	J	86°47'35"	27°51'32"	4005	R	MT	S
Shomare	K	86°48'40"	27°52'5"	4021	R	IS	N
Pangboche-Teouma	L	86°47'17"	27°51'32"	4148	R	MT IS	N
Imja confluence	M	86°49'08"	27°52'52"	4172	R	CP	Y
Khumbu confluence	N	86°49'05"	27°52'59"	4172	R	CP	Y
Pheriche hydro	O	86°49'08"	27°53'13"	4216	R	IS	Y
Pheriche village	P	86°49'16"	27°53'46"	4260	P R	MT IS	Y
Dingboche village	Q	86°50'06"	27°53'35"	4370	R	IS	Y
Dingboche hydro	R	86°50'28"	27°53'46"	4372	R	IS	Y
Tauche Kharka	S	86°47'17"	27°52'23"	4405	R	IS	S
Phulung Kharka	T	86°49'01"	27°54'36"	4504	R	IS	S
Tukla	U	86°48'54"	27°55'59"	4700	R	IS	Y
Chukung	V	86°52'41"	27°54'04"	4752	R	CP	Y
Lobuche river	W	86°48'50"	27°57'25"	4840	R	IS	Y
Lobuche spring	X	86°48'43"	27°57'18"	4935	R	IS	S
Imja Lake	Y	86°54'29"	27°54'00"	5001	R	MT	Y

(+) precipitation samples are in gray; the others are river samples.
 (++) see location in [Figure 1](#)
 (*) Data type: P=precipitation; R=river
 (**) Sample: MT=major/trace + conductivity/pH; IS=isotopes; CP= only conductivity/pH
 (***) Glacier: N=no; Y=yes; S=not significant

853

854 Table 2. Main characteristics of the geochemical samples: water temperature, pH, electrical conductivity, and major ions.

Name (+)	Label (++)	Var (*)	WT °C	pH	EC µS/cm	HCO ₃ ⁻ mg/L	Cl ⁻	NO ₃ ⁻	SO ₄ ⁻	CA ⁺⁺	Mg ⁺⁺	Na ⁺	K ⁺	SiO ₂
Pang.-Teouma	L	M	7.2	7.3	13.7	6.37	0.13	0.62	1.85	1.46	0.17	0.80	0.29	4.86
		sd	3.4	0.2	1.7	0.64	0.05	0.30	0.32	0.18	0.04	0.16	0.11	0.82
Pang.-Kisang	I	M	9.7	7.3	15.4	7.46	0.30	0.46	1.85	1.56	0.19	1.11	0.36	4.93
		sd	3.6	0.2	3.2	1.58	0.23	0.26	0.26	0.18	0.04	0.49	0.12	1.17
Pang.-Tauche	J	M	9.0	7.5	42.5	12.27	0.12	0.82	9.41	5.99	0.57	0.96	0.39	4.46
		sd	3.9	0.2	7.8	4.35	0.03	0.23	2.17	1.44	0.09	0.14	0.05	0.63
Pang.-Imja	G	M	7.5	7.7	45.0	20.16	0.20	0.53	6.73	7.50	0.37	1.02	0.85	10.56
		sd	3.0	0.1	9.1	4.49	0.12	0.54	1.24	1.45	0.06	0.43	0.13	6.12
Pang.-Chomar	H	M	8.7	7.4	22.4	15.31	0.12	0.34	0.68	3.68	0.23	0.97	0.28	5.93
		sd	2.3	0.3	7.8	5.21	0.03	0.22	0.20	1.13	0.06	0.37	0.07	1.93
Pang.-Chomar bottled water	H			8.6	29.3	15.75	0.44	1.38	0.54	4.87	0.16	0.43	0.19	8.19
Imja Lake	Y			7.0	30.0	9.86	0.37	1.52	6.28	3.90	0.24	0.71	0.73	1.61
Pheriche hydro	O			7.4	62.6	27.70	1.02	0.24	0.47	8.60	0.22	1.10	1.31	2.04
Pheriche village	P			6.2		14.16	0.29	0.79	8.38	2.77	0.17	0.57	1.53	0.07

(+) precipitation sample is in gray; the others are river samples.

(++) see location in [Figure 1](#)

(*) M = mean; sd = standard deviation

WT = water temperature EC = electrical conductivity

855

Water Geochemistry of Mount Everest

856 Table 3. Average concentrations of trace elements.

Name (+)	Label (++)	Var (*)	Li	B	Al	Ti	Cr	Mn	Fe	Ni µg/L	Cu	Zn	Rb	Sr	Cs	Ba	Pb	U	
Pang.- Teouma	L	M	0.34	0.60	36.6	1.36	0.16	0.64	20.4	0.93	0.26	1.57	1.32	3.42	0.21	1.05	0.02	0.81	
		sd	0.06	0.15	23.0	1.44	0.11	0.69	19.0	1.31	0.07	1.92	0.29	0.45	0.05	0.50	0.02	0.26	
Pang.- Kisang	I	M	0.41	0.77	68.0	3.09	0.18	1.07	50.6	0.95	0.41	2.60	1.53	3.74	0.19	1.25	0.14	0.81	
		sd	0.10	0.18	33.0	2.70	0.06	0.71	36.7	1.57	0.11	1.60	0.22	0.51	0.06	0.25	0.08	0.23	
Pang.- Tauche	J	M	0.80	1.21	34.9	2.35	0.14	0.52	29.2	1.18	0.31	1.51	1.63	8.89	0.59	0.82	0.03	5.75	
		sd	0.12	0.19	23.6	1.96	0.15	0.34	23.8	1.44	0.10	1.42	0.23	2.02	0.11	0.21	0.02	2.36	
Pang.- Imja	G	M	18.88	4.19	2365.6	205.79	4.28	56.86	3019.4	4.27	4.16	11.15	18.46	15.78	4.74	17.07	2.40	10.96	
		sd	13.25	1.47	2325.6	173.57	3.83	61.78	2616.1	2.58	4.58	9.14	15.72	3.26	4.28	17.24	2.35	3.78	
Pang.- Chomar	H	M	0.35	0.59	35.9	1.57	0.54	0.60	23.2	0.47	0.26	2.00	1.25	6.73	0.28	0.74	0.04	1.11	
		sd	0.07	0.13	20.4	1.51	0.67	0.45	17.8	0.73	0.07	1.12	0.34	2.30	0.10	0.16	0.03	0.20	
Imja Lake	Y		4.76	1.92	9.7	na	0.03	1.19	7.4	0.06	0.09	1.81	1.33	3.86	0.14	0.53	0.04	0.11	
Pheriche hydro	O		9.40	2.69	8.6	na	0.04	6.32	3.1	0.05	0.10	3.08	2.62	28.96	0.34	0.69	0.03	0.20	
Pang.-Chomar bottled water	G		0.49	LOD	11.2	na	0.03	0.09	1.2	0.03	0.05	19.61	0.09	6.36	0.01	0.74	0.07	0.82	
Pheriche village	P		0.10	0.76	5.5	na	0.10	1.46	1.5	0.10	0.20	5.85	1.97	5.30	0.02	1.63	0.10	0.02	
(+) precipitation sample in grey; the others are river samples (++) see location in Figure 1 (*) M= mean; sd = standard deviation; LOD = limit of detection; na = not available																			

857

858 Table 4: Main characteristics of the stable isotope river samples

Name	Label (+)	Alt. (m)	Sampling seasons (*)						Isotope data				
			N14	MH15	N15	MY16	N16	MY17	mean ¹⁸ O	mean D	max dif. ¹⁸ O	max dif. D	mean d-excess
Kharikhola	A	1981				X	X	X	-10,16	-66,9	0,40	5,4	14,4
Phakding	B	2620		X	X	X	X	X	-15,89	-114,87	0,47	2,9	12,2
Jorsalle	C	2850		X	X 2		X	X	-16,05	-116,3	0,34	2,1	12,1
Pangom river	D	2880	X	X		X		X	-11,71	-80,5	5,98	53,6	13,2
Phunki Tenga	F	3200		X	X	X	X	X 2	-16,54	-120,5	0,20	0,1	11,8
Pangboche-Imja	G	3917			X	X	X	X	-16,67	-120,7	0,22	2,5	12,6
Pangboche-Tauche	J	4005	X	X	X	X	X	X	-15,51	-113,7	1,65	10,9	10,3
Shomare	K	4021	X		X				-14,08	-107,2	0,53	0,7	5,6
Pangboche-Teouma	L	4148			X	X	X		-14,6	-107,8	1,70	10,8	8,9
Pheriche hydro	O	4216			X	X	X	X	-16,7	-121,7	0,39	2,29	11,9
Pheriche village	P	4260	X						-16,55	-122,8			9,6
Dingboche village	Q	4370	X		X	X		X	-16,83	-121,7	0,57	5,2	12,9
Dingboche hydro	R	4372	X 2						-17,63	-132,2	0,03	0,7	8,8
Tauche Kharka	S	4405				X			-14,51	-104,7			11,4
Phulung Kharka	T	4504	X 2						-17,13	-127,9	0,10	0,47	9,2
Tukla	U	4700	X		X				-18,21	-133,93	0,35	3,84	11,8
Lobuche river	W	4840	X 2						-16,71	-123,03	0,21	0,1	10,7
Lobuche spring	X	4935			X				-15,06	-109,9			10,5

(+) see location in [Figure 1](#)
 (*) Axx: A=M (monsoon) or (extra-monsoon); xx is the year (e.g., 14 = 2014)
 N14, November 2014; MH15, March 2015; N15, November 2015; My16, May 2016, N16, November 2016
 My17, May 2017.

859

860 Table 5: Additional observations of electrical conductivity, performed on 19, 21, and 22 June 2012.

Name	Label (+)	Electrical conductivity ($\mu\text{S}/\text{cm}$)
Pangboche-Imja	G	53.0
Khumbu confluence	N	67.6
Pheriche hydro	O	62,6
Imja confluence	M	35.4
Dingboche hydro	R	32,9
Chukung	V	41.5
Imja Lake (*)	Y	29,7
		30,7
		29,6

(+) see location in [Figure 1](#)
 (*) 3 different sampling points in the outlet narrows.

861